UNIVERSITY OF MINNESOTA
ST. ANTHONY FALLS HYDRAULIC LABORATORY

Technical Paper No. 49, Series B

Measurements of the Unsteady Force on Cavitating Hydrofoils in a Free Jet

by
C. S. SONG

Prepared for
OFFICE OF NAVAL RESEARCH
Department of the Navy
Washington, D.C.
under
Contract Nonr 710(24), Task NR 062-052

June 1964
Minneapolis, Minnesota

UNIVERSITY OF MINNESOTA
ST. ANTHONY FALLS HYDRAULIC LABORATORY

Technical Paper No. 49, Series B

Measurements of the Unsteady Force on Cavitating Hydrofoils in a Free Jet

by
C. S. SONG

Prepared for
OFFICE OF NAVAL RESEARCH
Department of the Navy
Washington, D.C.
under
Contract Nonr 710(24), Task NR 062-052

June 1964
Minneapolis, Minnesota

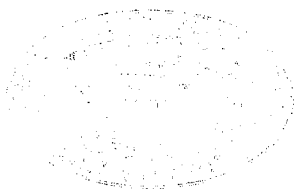

ABSTRACT

Experimental data concerning force and other related quantities associated with unsteady supercavitating flow about bodies tested in a free-jet water tunnel are reported herein. Three types of unsteady flows were studied -- those due to pitching oscillation, sudden ventilation, and sudden angle of attack change. All test bodies were of such geometrical configuration that separation could occur only at two or three fixed points.

The first type of unsteady flows was subdivided into three categories, each having different characteristics. When a flat plate was oscillated about a large mean angle of attack at small cavitation number and without ventilation, the cavity pressure remained unchanged. When air was supplied to the cavity for ventilation, the cavity pressure oscillated with the same frequency as that of the body oscillation. When the plate was oscillated about a small mean angle of attack, there was a change in the cavity configuration even without ventilation and the resulting flow was quite irregular. The plate was oscillated at the maximum reduced frequency of 0.03.

The second phase of the experiment involved measurements of cavity pressure, cavity length, and the force on the body following a sudden ventilation of an otherwise steady cavity. It was found that the change in cavity length and the change in the force lagged behind the cavity pressure change. Furthermore, the rate of cavity increase never exceeded the free-stream speed.

An attempt was also made to measure the response of the flow to a sudden angle of attack change. It was concluded that, due to the oscillatory nature of the cavity, a faster angle of attack change than was attained in the experiment is needed to obtain a useful unit function response curve.

CONTENTS

LIST OF ILLUSTRATIONS

MEASUREMENTS OF THE UNSTEADY FORCE ON CAVITATING HYDROFOILS IN A FREE JET

I. INTRODUCTION

The continuing development of hydrofoil craft and supercavitating propellers over the past several years has resulted in considerable advancement in cavity flow theory. Nevertheless, due to its inherent difficulties, the mechanism of unsteady cavity flows has not been completely understood. It has become apparent for some time that good experimental data are urgently needed.

In recent years, the St. Anthony Falls Hydraulic Laboratory has been engaged in an experimental study of unsteady supercavitating flow problems under the sponsorship of the Office of Naval Research of the United States Navy. The types of unsteady supercavitating flows studied include flow produced by an oscillating foil, flow due to sudden air supply into the cavity, and flow due to sudden angle of attack change. The first type of problem is directly related to the problem of hydrofoils moving under a surface wave and its solution is also useful in flutter analysis. The second type of problem is applicable to hydrofoil boat control. When a hydrofoil is moving at an intermediate speed, which is too low for a natural supercavity to be formed but too high to have fully wetted flow, it may be necessary to create a supercavity by means of ventilation. Sometimes ventilation may also be desirable for noise reduction purposes, [1].* Since a steady ventilated cavity flow requires a constant ventilation rate, any change in ventilation rate will result in an unsteady flow. This type of the unsteady flow is the concern of the second phase of the experiments reported herein.

Provided the system is linear, the response of the flow to an arbitrary change in hydrofoil characteristics may be synthesized using either the harmonic responses or the unit step function response. To explore the possibility of using the latter method, a limited number of experimental data were also obtained for the flow due to sudden change in the angle of attack.

---

*Numbers in brackets refer to the List of References on page 21.

The present report is based mainly on experimental data taken in the free-jet tunnel prior to the summer of 1963. A two-dimensional wedge and flat plate were used as test bodies.

This research has been supported by the Office of Naval Research of the United States Department of the Navy under Contract Nonr 710(24) Task NR 062-052. The author wishes to acknowledge the contribution of Messrs. John Almo and John Kolodnycki, who were responsible for the design and maintenance of various test facilities and Messrs. Paul T. Edstrom, R. A. Rao, and Frank Yu-Fang Tsai, who were responsible for the experimental details. Special thanks is due to Prof. Edward Silberman for his helpful discussion and guidance. The manuscript was prepared for printing by Mrs. Kathleen Lagerberg.

II. EXPERIMENTAL APPARATUS

The experimental studies were conducted in the two-dimensional gravity-flow, free-jet water tunnel at the St. Anthony Falls Hydraulic Laboratory. The tunnel is a free-falling, nonrecirculating type utilizing river water and having a vertical test section. This tunnel has two principal features that make it especially useful for the type of investigation reported herein. First, very low cavitation numbers can be obtained without blockage; and second, large quantities of air can be added to a cavity without having to remove the air from the tunnel water subsequently. Furthermore, the test section is completely transparent, except where a dynamometer is located, facilitating visual observation and photography. A front view of the tunnel in operation is shown in Fig. 1.

The test section is designed to produce a rectangular jet 5 in. thick and of variable width ranging from 6 to 12 inches. All the data reported hereafter were taken in the 10-in. jet unless otherwise stated. The jet is bounded by two solid walls and two free surfaces. The working velocity of the jet is between 20 fps and 50 fps. Any pressure between vapor pressure and a pressure slightly lower than atmospheric pressure can be created at the test section. The free-jet tunnel and the methods of velocity and ambient pressure measurement are descirbed in detail in Ref. [2]. Fifty-inch mercury manometers were used for both average cavity pressure and average

ambient pressure measurements and for measuring their differences. Electronic strain gage type pressure transducers made by Consolidated Electrodynamic Company were used for transient pressure measurements. Natural frequencies of the transducers were over 4 KC per second in air. Pressure transducers were always placed right at the point of interest to minimize the dynamic effect of a fluid column.

No provision was made to determine the air content of the river water used as test fluid. The effect of air content in the water is considered to be of secondary importance for the type of experiment reported herein.

Two identical strain-gage type dynamometer units, specifically designed for the experimental program, were mounted at opposite points on the test section walls. The strain gages were mounted in pairs on sets of "lift" beams and "drag" beams. A 5-in. span test body was suspended between these units by means of retractable pins. Test bodies were so constructed that the centerline of a wedge or the pressure side of a flat plate surface was aligned with a pair of the drag beams. At non-zero attack angle, the true lift and drag are related to the dynamometer reading by the following pair of equations.

$$\begin{aligned} L &= L' \cos \alpha - D' \sin \alpha \\ D &= D' \cos \alpha + L' \sin \alpha \end{aligned} \tag{1}$$

where L and D are lift and drag, L' and D' are the dynamometer readings, and α is the angle of attack.

A driving mechanism was attached to the dynamometer housing so that a test body and the dynamometer could be rotated together while the water tunnel was in operation. The body-dynamometer unit could be oscillated at a maximum amplitude of 15 degrees and at a maximum frequency of 3 cps at relatively small amplitude. Alternately, a sudden change in angle of attack from one fixed value to another could be produced. The dynamometer was designed to measure a transient force of frequency up to 100 cps; the frequency of the primary mode of vibration of the system in air with the 2-in. flat plate test body was determined to be approximately 170 cps. A detailed description of the dynamometer may be found in Ref. [3].

III. TEST RESULTS

A. Oscillating Foil

A 2-in. flat plate and a 1-in. wedge with 15 degree vertex angle were used as test bodies in this phase of the experimental program. For reference purposes and to check the functioning of the equipment, steady flow measurements were first taken in a 10-in. jet.

Figure 2 shows the result of the cavity length measurement for the flat plate at three different angles of attack. Here the cavity length is defined as the distance between the leading edge of the plate and a point at the rear end of the cavity where the white cloud of gas-water mixture appeared to be thinnest. It was observed that the cavity length thus defined fluctuated about an apparent mean value even when the flow was kept as steady as possible. The values plotted in the figure are the estimated mean values which may contain errors as high as one inch or even more. The cavitation number is defined as

$$\sigma = \frac{P_\infty - P_c}{\frac{1}{2}\rho V^2} \tag{2}$$

where P_∞ = ambient pressure surrounding free jet,
P_c = measured cavity pressure,
ρ = density of water, and
V = ambient velocity with test body removed.

An alternate definition of the cavitation number, σ_v, wherein the vapor pressure is used in place of the measured cavity pressure is sometimes more convenient than the definition given by Eq. (2).

Figure 3 shows the corresponding lift and drag coefficients using the pressure side of the surface as reference area. Skin friction drag was estimated and subtracted from the drag data before plotting. Corrections due to the tunnel wall effect and other secondary flows were neglected. Theoretical lift and drag coefficients by Silberman [4] for zero cavitation number, are also indicated in the figure. The agreement between the theory and experiment is good. To show the variation of C_L and C_D for a wider range of

cavitation numbers, another set of data including non-cavitating, partially cavitating and supercavitating conditions, were taken at $\alpha = 10.5^{\circ}$ and the data are plotted in Fig. 4; the abscissa in this figure is cavity length. (Note that the values of $C_L/2\pi\alpha$ and $C_D/2\pi\alpha^2$ for non-cavitating conditions are very close to unity, the limiting value from thin-airfoil theory, while their limiting values for very long cavities are both approximately equal to 0.2, Silberman's theoretical value.)

(1) Oscillation at Large Angle of Attack

The 2-in. plate was oscillated between 13 and 21 degree angle of attack at various supercavitating flow conditions. Oscillographic records of lift, drag, angle of attack, and cavity pressure were taken for each run. Samples of the records are shown in Fig. 5.

Figure 5a is for a natural cavity; there was no external air supply to the cavity except possibly for a small quantity that may have leaked in. It is seen that a nearly perfect harmonic oscillation of the plate was achieved, although at low frequency. The resulting lift and drag curves were also nearly harmonic with no observable phase shift. As may be expected, the cavity pressure remained almost constant and only slightly larger than the vapor pressure. The high frequency and small amplitude hash are believed to be due to flow noise and other vibrations which are of no concern to the current investigation.

Figure 5b shows similar data for a lightly ventilated cavity. A characteristic of the ventilated cavity shown by the record is that the cavity pressure oscillates about its mean value almost anti-symmetrically with the angle of attack oscillation. With somewhat larger air supply, the cavity would pulsate if the angle of attack were kept constant at 13 degrees (left side of Fig. 5c). Pulsations disappear if the foil is oscillated (right side of Fig. 5c). Finally, Fig. 6 shows that with large air supply rate, the cavity about an oscillating foil may also pulsate. The dimensionless numbers appearing in these and the following figures are defined as follows:

$$C_L = \frac{\text{Lift}}{\frac{1}{2}\rho V^2 CS} = \text{lift coefficient}$$

$$C_D = \frac{\text{Total drag - Skin friction}}{\frac{1}{2}\rho V^2 CS} = \text{drag coefficient}$$

$$C_A = \frac{W_A}{\gamma_A VCS} = \text{air supply coefficient}$$

$$k = \frac{\omega C}{2V} = \text{reduced frequency}$$

where C = chord,
S = span,
ω = angular speed of oscillation,
W_A = weight rate of air flow at room condition, and
γ_A = specific weight of air at room condition.

Figure 7 shows the data for the instantaneous lift coefficient when the plate oscillated between 13 and 21 degree attack angle at the reduced frequency, k, of about 0.005 with variable air supply coefficient. The corresponding data for the drag coefficient are shown in Fig. 8. The skin friction was roughly estimated assuming turbulent boundary layer flow and was a very small part of the total drag in any event. It is seen that the ratio of the lift coefficient to the drag coefficient was approximately equal to tan α for all cases, as may be expected for the supercavitating flat plate.

Examination of the records shown in Figs. 5 and 6 for $C_A > 0$ reveals that the cavity pressure curves are not exactly anti-symmetric with respect to the angle of attack curve. They are somewhat skewed with a tendency for the maximum and the minimum cavity pressure to occur sometime after the minimum and the maximum angle of attack, respectively. The phase difference between the maximum cavity pressure and the minimum angle of attack, ϕ_1, and that between the minimum cavity pressure and the maximum angle of attack, ϕ_2, for a constant k (0.0055) and nearly constant ambient conditions are plotted as functions of C_A in Fig. 9. For the flow conditions tested, there is a maximum value of ϕ_1, occurring near $C_A \approx 4 \times 10^{-3}$.

The data shown in Fig. 7 may be used to compute the average lift curve slope, $\Delta C_L/\Delta\alpha$, and the average rate of cavitation number change per unit

angle change $\Delta\sigma/\Delta\alpha$. The results, for a constant reduced frequency (k = 0.0055) but variable air supply coefficient, are shown in Fig. 10. It is readily seen that both $\Delta C_L/\Delta\alpha$ and $\Delta\sigma/\Delta\alpha$ increase with increasing air supply coefficient.

All the data for C_L in Fig. 7 corresponding to $\alpha = 13^\circ$ and $\alpha = 21^\circ$ are plotted as a function of σ on a single graph in Fig. 11. The mean value of the steady flow lift coefficient for $\alpha = 13^\circ$ is estimated from Fig. 3a and shown on the same graph as a solid line. It is interesting to note that the line representing the steady flow data agrees fairly well with the unsteady flow data. The scatter of the unsteady flow data is also comparable to that of the steady flow data. It may now be hypothesized that, at a very low reduced frequency, although the cavity pressure behind an oscillating plate with a constant ventilation rate varies with time, the instantaneous lift coefficient may be determined by using the steady flow relation provided that the instantaneous values of attack angle and cavitation number are used.

An attempt was also made to study the effect of frequency on force and cavity pressure. For this purpose, the test body was oscillated at different frequencies while the ventilation rate was kept constant. Figure 12 shows the data for lift and drag coefficients when the air supply coefficient, C_A, was kept approximately equal to 6.3×10^{-3}. The maximum reduced frequency attainable in the apparatus was only 0.032. For ventilated cavities, the amplitude of cavity pressure and lift coefficient oscillations were found to depend on the frequency of the foil oscillation. The amplitude per unit attack angle change for a constant air supply coefficient, $C_A \approx 6.3 \times 10^{-3}$, are plotted as functions of the reduced frequency in Fig. 13. It is seen that both lift curve slope and the rate of cavitation number change are decreasing functions of reduced frequency. Also, at moderately high reduced frequency, $K > 0.012$, the amplitudes of the cavitation number and the lift coefficient oscillations are almost independent of the reduced frequency.

(2) Oscillation at Small Angle of Attack

The experiment described in the last section involved no major change in the cavity configuration; there always existed a supercavity with fixed

separation points. When a foil was oscillated about a small attack angle, major changes in the cavity configuration took place during each cycle of oscillation. All the data taken in this connection are for the 2-in. flat plate with natural cavity.

For the purpose of comparison, steady flow data for five different angles of attack were taken. The measured steady flow lift coefficient data are summarized and plotted as a function of cavitation number in Fig. 14. The cavitation number is based on vapor pressure in this and the following figures since the cavities disappeared in some cases so that cavity pressure was not always measurable.

When the foil was set at 8 degree angle of attack no unusual flow behavior was observed. The leading edge cavity first appeared when σ_v was lowered to approximately 1.4. Further reduction of σ_v was followed by increased cavity length and lift coefficient and the latter reached its maximum value when the cavity became nearly as long as the chord. For smaller angle of attacks, however, different phenomena were observed. The observed flow characteristics are described for the cases of $\alpha = 6^\circ$, $\alpha = 4^\circ$, and $\alpha = 2^\circ$.

$\underline{\alpha = 6^\circ}$

For the sake of clearness, the experimental data for $\alpha = 6^\circ$ are singled out from Fig. 14 and replotted in Fig. 15. Schematic drawings of the cavity configurations corresponding to some representative data points are also included in the figure. It may be seen that, when the cavitation number was gradually decreased from a large value, a cavity first appeared at the leading edge (sketch "a"). Another cavity could also appear at the apex (see sketch "b") if σ_v was further reduced. The flow was very unstable within a considerable range of σ_v wherein different cavity configurations could be observed. The leading edge cavity fluctuated to the extent that the two cavities joined to form a single large cavity (sketch "c") for part of the time. The resulting flow looked somewhat like the oscillating cavity recently reported by Wade [5]. When the cavity fluctuated, the lift force also changed. It is seen in Fig. 15 that a single large cavity corresponded to the larger lift and the double cavity condition corresponded to the smaller lift. When σ_v was reduced below 0.6 only a single supercavity was obtained.

$\alpha = 4^{\circ}$

The lift coefficient data for 4 degree angle of attack shown in Fig. 14 are replotted in Fig. 16. At this angle of attack, the apex cavity appeared first when cavitation number was at approximately 1.35, (sketch "a"). With a slight drop in the cavitation number, approximately at 1.17, the leading edge cavity also appeared, as usual, on the suction side (sketch "b"). When the cavitation number was decreased further, the apex cavity continued to grow while the leading edge cavity remained relatively unchanged until a point indicated by sketch "c" is reached. At this point, the leading edge cavity switched from the suction side to the pressure side intermittently. As indicated by sketches "f" and "g", the suction side cavity was associated with a higher lift than the pressure side cavity. This unstable condition occurred only in a narrow range of cavitation number, $0.25 < \sigma_v < 0.35$. At a somewhat lower σ_v, the leading edge cavity remained on the pressure side, but its size fluctuated (sketches "h" and "i"). It should be noted that the shifting of the leading edge cavity was not necessarily followed by a shift in lift force direction. Only when σ_v was less than 0.16 did the pressure side cavity result in negative lift (sketches "h" and "i").

$\alpha = 2^{\circ}$

The lift coefficient data for this case are shown in Fig. 17. At this small angle of attack, the apex cavity appeared earlier ($\sigma_v = 1.73$) than in the previous cases as σ_v was lowered. The apex cavity continued to grow as σ_v was lowered. The leading edge cavity appeared first at the suction side when σ_v reached 1.1 (sketch "b"). This point corresponded roughly to the point of maximum lift coefficient. As may be expected, the leading edge cavity disappeared when σ_v was lowered slightly under 1.1. There was a considerable range of σ_v wherein no leading edge cavity could be observed. Finally, approximately at $\sigma_v = 0.5$, the leading edge cavity reappeared, this time on the pressure side (sketch "f"). By this time, the apex cavity had extended beyond the trailing edge of the plate. Further reduction of σ_v beyond 0.5 resulted in the growth of both cavities. The leading edge pressure side cavity fluctuated causing the lift coefficient to change by as much as 0.1 for a given σ_v. The lift coefficient always remained negative when σ_v was less than 0.2. A double cavity condition with the leading edge cavity extending to the mid chord and the apex cavity extending two or three chords beyond the trailing edge of the plate was observed (sketch "h"). At $\sigma_v = 0.14$ a single supercavity condition as indicated by sketch "i" was realized. As

may be expected, the magnitude of the negative lift coefficient dropped slightly when σ_v was reduced to zero.

The existence of double cavities and the occurrence of the leading edge cavity on the pressure side were also reported by Parkin [6]. Some of the more important facts revealed concerning steady flow at small angle of attack are recapitulated below.

(a) Contrary to the familiar trend, the inception cavitation number of the apex cavity is a decreasing function of the attack angle.

(b) For a given angle of attack, the leading edge cavity may appear on the suction side or the pressure side depending on the cavitation number.

(c) Even when all the ambient flow conditions are kept constant, the leading edge cavity may not be steady. It appears that two alternate cavity configurations are possible for a given ambient flow condition.

Of course, it is doubtful that the ambient flow (jet) was actually maintained constant and it is possible that the slight unsteadyness of the ambient flow might be the cause of the cavity fluctuation. Further investigation concerning this matter has not been carried out.

After the steady flow investigation was completed, the foil was oscillated between $\alpha = 2^\circ$ and $\alpha = 8\text{-}1/2^\circ$ at various frequencies and cavitation numbers. All the tests were made under non-ventilated conditions. A typical oscillographic record ($\sigma_v = 0.163$, $k = 0.0119$) is shown in Fig. 18. It is seen that the lift and drag curves show considerable irregularities even though an almost harmonic angle of attack oscillation was achieved. A comparison of lift and drag coefficient for several cycles of oscillations indicated large differences from one cycle to the next. In fact, it was impossible to find two cycles showing identical results. Examples of two consecutive cycles showing the largest discrepancies were selected from Fig. 18 and plotted in Fig. 19. Similar data for two higher cavitation numbers are shown in Fig. 20. As may be seen from Figs. 19 and 20, the lift and drag curves corresponding to increasing α were almost always lower than those corresponding to decreasing α. Although part of this hysteresis could be due to the characteristics of the dynamometer, the dynamometer hysteresis

alone is far too small to account for the large change seen in Fig. 19b. That the trend shown in Fig. 19 is opposite to the trend shown in Fig. 7 (for large α with ventilation) also indicates that the hysteresis was due to the flow rather than to the dynamometer. It should be noted that zero lift coefficient corresponded roughly to minimum drag coefficient.

Observation of Fig. 19 and many other similar graphs revealed that the lift coefficient curves have three distinct slopes: minimum slope exists between $\alpha = 2^\circ$ and $\alpha = 3^\circ$ and maximum slope between $\alpha = 3^\circ$ and $\alpha \approx 6^\circ$. Unfortunately, a clear view of the cavity on the foil was blocked by the dynamometer and no attempt was made to take motion pictures of the cavity. However, the steady flow data as shown in Figs. 15, 16, and 17 suggest that a full single cavity might exist for $\alpha > 6^\circ$ and suction side double cavities might exist for $3^\circ < \alpha < 6^\circ$. The minimum slope might correspond to a pressure side leading edge cavity or even to flow without a leading edge cavity. Average lift curve slopes corresponding to $\alpha > 6^\circ$ and $3^\circ < \alpha < 6^\circ$ for $\sigma_v = 0.163$ are plotted in Fig. 21 as functions of k. Slight effect of k, especially for a single full cavity region, is indicated.

Finally, the performance of the oscillating foil is compared with that of a stationary foil in Fig. 22. Figure 22a shows the average lift coefficient as a function of α. It should be noted that, due to the instability of the cavity configuration discussed earlier, the steady flow curve as indicated by solid lines has branches. Since the unsteady flow data lie nearer to the lower branch of the steady flow data and, since, the lower branch indicated shorter leading edge cavities, it is suggested that the oscillation tended to shorten the cavity. The same data are plotted in a polar form in Fig. 22b. It is clearly indicated that the oscillating foil at small α is substantially inferior to the stationary foil at the same C_L.

B. Sudden Change in Cavity Pressure

It is well known that the cavity pressure of a natural cavity is generally only slightly larger than the vapor pressure. The pressure in a steadily ventilated cavity is a variable depending on the air supply coefficient and other factors. When a natural cavity is suddenly ventilated, the flow shortly after the ventilation begins is unsteady; cavity pressure and cavity size increase while lift and drag decrease.

For the purposes of this experiment, a 280-cubic in. air tank was used as the source of air supply. The air tank was placed near the test section and connected to the rear end of the test body by a short pipe equipped with a gate valve. A strain gage type pressure transducer was attached to the air tank for the purpose of measuring instantaneous tank pressure.

(1) Cavity Length and Cavity Pressure

A 3/16-in. normal plate and a 1-in. symmetrical wedge with 28 degree vertex angle were tested for the purpose of studying the effect of sudden ventilation on cavity length and cavity pressure. Since the presence of the dynamometer would partially obstruct the view of the cavity near the foil, it was found desirable to replace the dynamometer with a lucite block. The variation of cavity size and cavity shape was recorded by means of motion pictures. Instantaneous cavity pressure was measured using a strain gage type pressure transducer placed on the tunnel wall approximately one inch downstream of the trailing end of the test body. For the purpose of synchronization, arbitrary time origins were marked simultaneously on the pressure record and the movie film.

Figure 23 shows two typical records of the tank pressure and the cavity pressure changes obtained for a 3/16-in. normal plate operated at $\sigma_v \approx 0.4$. It is readily observed that the tank pressure reduced almost uniformly during the initial stage indicating almost constant ventilation rate. On the contrary, the cavity pressure increased very rapidly at the initial instant and less rapidly thereafter. Record (a) also shows that the cavity pressure may oscillate about a mean value indicating the beginning of pulsation as reported in Ref. [7] and [8]. After most of the air in the tank was expended, the mean cavity pressure as well as the amplitude of the cavity pressure oscillation gradually decreased until the cavity ceased to pulsate and the original natural cavity was reproduced. For a larger initial tank pressure or a larger valve opening, as represented by record (b), the cavity eventually grew too long and split ($\sigma \approx 0$ for the split cavity).

The variation of cavity length due to sudden ventilation measured for the 3/16-in. normal plate at $\sigma_v \approx 0.4$ is shown in Fig. 24a. The four curves at the left side of the graph are for the initial stage of ventilation.

It is seen that the cavity grew very slowly at the initial instant, but the rate of growth increased very rapidly and maximum rate is reached within a short time (of order of 0.05 second). As may be expected, the rate of cavity growth is an increasing function of air supply rate. The maximum rate of cavity length increase obtained from the first curve in Fig. 24a is 14.4 fps, which is considerably less than the ambient water speed of 41 fps. To obtain data for faster expansion rate, the 28 degree wedge of 1 in. length equipped with a larger air pipe was tested at approximately the same σ_v. The test result is shown in Fig. 24b. A maximum cavity growth rate of approximately 40 fps, very close to the water speed, was achieved. With the present system, a growth rate greater than the water speed was not realized. It is conjectured that the cavity length can not grow faster than the ambient water speed unless the cavity pressure is raised above the ambient pressure as in the case of rocket propulsion. Attention is called to the onset of an instability at high ventilation rate as evidenced by the first curve in Fig. 24b.

Curve No. 5 in Fig. 24a is typical of the curves at a later stage of ventilation when tank air is nearly exhausted. It was found that the curve is almost independent of the initial ventilation rate.

To show the relationship between cavity length and the instantaneous cavitation number, the first four curves in Fig. 24a and those in Fig. 24b are replotted in Fig. 25 using σ as the independent variable. The accuracy of data plotted in this figure depends critically on the synchronization of the film and the pressure record. The possible error involved in the estimation of the time origin was about 0.01 second. Allowing for the uncertainties involved, it is reasonably well established that the cavity length change lagged behind the cavitation number change. The lag is more evident for high ventilation rates.

An attempt will now be made to correlate these sudden ventilation data. Since the time involved in the initial stage of ventilation is small, the amount of air escaping from the cavity due to diffusion should be negligibily small compared with the air retained in the cavity. Assuming a barotropic flow and assuming that the cavity volume is proportional to the n-th

power of the cavity length, the law of conservation of air mass leads to

$$\frac{P_o^{1/\kappa} - P_t^{1/\kappa}}{P_c^{1/\kappa}} = K\ell^n \qquad (3)$$

where P_o = initial air tank pressure,
P_t = instantaneous air tank pressure,
P_c = instantaneous cavity pressure,
ℓ = cavity length,
κ = a gas constant, and
K, n = correlation constants.

Although there should be some frictional loss in the gas flow, for the sake of simplicity the flow is assumed to be isentropic and κ is taken to be 1.4. Figure 26 shows the correlation of the data from Fig. 24a plotted in accordance with Eq. (3) on log-log paper. Fairly good correlation for cavities longer than 10 in. is apparent. It should also be noted that, according to the figure, the empirical exponent n is approximately equal to 1.6. This value is very close to the well known theoretical value for long steady cavities, $n = 1.5$.

(2) Lift and Drag

The 2-in. flat plate foil was tested in a 10-in. jet at 11 degrees angle of attack for the purpose of studying the effect of sudden ventilation on lift and drag. Figure 27a is a typical record of lift, drag, cavity pressure, and the air tank pressure for a relatively large ventilation rate. The cavity pressure transducer was placed 6 in. downstream of the leading edge of the foil in order to clear the dynamometer. For this reason, only the pressure in a cavity longer than 6 in. could be measured and the record for the initial instant of ventilation was missing. Figure 27b is a similar record for a smaller ventilation rate where it was possible for the cavity to pulsate.

The variation of the cavitation number and the lift coefficient with time shortely after sudden ventilation are plotted in Figs. 28a and 28b, respectively. Figure 29 is a cross plot of C_L as a function of σ. It seems

that, for high ventilation rate, the change of C_L lagged behind the σ change. Even allowing for a possible error of about 0.01 second in the determination of the time origin, the trend is clearly indicated. There is no theory available at the present time to check this experimental result.

C. Sudden Change in Angle of Attack

For this experiment, the foil-dynamometer unit was geared to a shaft and a pulley from which a weight was suspended. The pulley was so designed that upon releasing the locking mechanism the shaft would rotate under the action of the weight and stop at a preassigned angle. A braking force was provided by a mechanical stop. The speed of rotation could be changed by changing the suspended weight. The angle of attack was calibrated against the angular position of a shaft attached to a gear situated midway between the pulley and the dynamometer.

The 2-in. flat plate hydrofoil was tested at natural supercavitating conditions. The plate could be rotated from 14 degree to 7 degree attack angle at the maximum angular speed of 40 degrees per second. Using a relatively small weight, a quite long period of constant angular speed could be obtained. On the other hand, a larger weight would result in a more extended period of angular acceleration and a shorter period of constant speed.

Some oscillographic records of changing angle of attack and instantaneous forces are shown in Fig. 30. A sharp break in the slope of the angle of attack curves at $\alpha = 7^\circ$ indicates a large angular deceleration. The maximum angular deceleration was estimated to be about 300 rad. per sec.^{2} which corresponds to a linear deceleration of nearly one g at the leading edge of the foil. However, since the period of the maximum deceleration was of the same order of magnitude as the natural period of the system (0.0059 second), the virtual force could not be registered. Most records, with a few exceptions such as Fig. 30c, showed immediate response of lift and drag to the sudden stop. The reason for the peculiarity of the lift and drag curve following the sudden stop in record (c) was not determined although the opposite trends shown by the lift and drag curves suggests that a change in the relative orientation of the foil and the dynamometer might be the reason. The foil was attached to the dynamometer by means of three pins at each end of

the foil; loose pins might have permitted the foil to rotate with respect to the dynamometer.

If the system is linear, it is of great practical importance to determine the unit step function response to a sudden attack angle change. The response of the system to an arbitrary attack angle change may, then, be obtained by integration. Since the records show almost linear inputs, they are considered ideal linear functions in the following analysis. It is well known that the response to a zeroth order unit step function input is equal to the first derivative of the response function due to a linear function input. The instantaneous lift coefficient was computed at successive instants 0.01 second apart. The first derivative of the lift coefficient, dC_L/dt, was computed by the method of finite differences using 0.05 second intervals. The reason for chosing a 0.05 second interval rather than 0.01 second for the numerical differentiation was to minimize the effect of vibration at natural frequency. The resulting unit step response function

$$C_o(t) = \frac{\partial C_L(\alpha, t)}{\partial t} \cdot \frac{\Delta T}{\Delta \alpha} \tag{4}$$

having the unit of per radian is plotted in Fig. 31. Symbols used in Eq. (4) have the following meanings.

$C_o(t)$ = zeroth order unit function response,
$C_L(\alpha, t)$ = instantaneous lift coefficient for linear α change, and
$\frac{\Delta \alpha}{\Delta T}$ = rate of change of attack angle.

For the purpose of comparison, the steady state lift curve slope for a supercavitating flat plate, assuming

$$C_L = \frac{2\pi \sin \alpha}{4 + \pi \sin \alpha} (1 + \sigma) \tag{5}$$

is also indicated in Fig. 31 for the terminal attack angles of 14 and 7 degrees. Equation (5) is the well known equation [9] for infinite fluid and infinite cavity adjusted to take into account the first order effect of σ. Theoretically, the response function at large t should agree with Eq.

(5). The agreement is fairly good if the large amplitude oscillation of the data at the frequency of an order of 10 cps is overlooked. The same type of oscillation was also found when α was kept constant. This is believed to be due to the oscillatory nature of the cavity length which may be observed even in a steady state condition. In fact, it was reported by Song and Silberman [1] that the frequency spectrum of the pressure fluctuation near a steady cavity always exhibited a peak in a low frequency range, $f < 60$ cps. Furthermore, the correlation of the intensity of the pressure fluctuation and the distance between the pressure transducer and the tail of the cavity enabled them to identify this peak with the cavity length fluctuation [1]. The apparent time lag of the response curve of approximately 0.095 second as shown in Fig. 31 was probably due to gaps between transmission gears rather than being an indication of a hydrodynamic property.

The amplitude of an oscillatory force at approximately 10 cps is so large that the usefulness of data shown in Fig. 31 is doubtful. Furthermore, it seems that the response time of the flow is less than 0.1 sec and, hence, a faster angular rotation ($T < 0.1$) is necessary for a better result.

Although the present investigation does not concern flutter phenomenon, it may be of interest to some readers to point out evidence of a finite amplitude flutter oscillation of approximately 170 cps in Fig. 30. There were many similar records. This frequency is of the same order of magnitude as the natural frequency of the system in air. A sudden growth followed by a decay of the oscillation, apparently excited by the sudden deceleration of the foil as shown in the last record of Fig. 30 is noteworthy. A similar sudden burst of vibration could also take place without apparent external excitation as may be observed near the left hand edge of record (b) in the same figure.

IV. CONCLUSIONS

Unsteady supercavitating flows around a foil were generated by pitching oscillation, sudden ventilation, and sudden attack angle change. The response of the flow to the specified changes in the ambient condition were measured. As a result of the present investigation, the following conclusions are offered.

A. Oscillating Foil

The following conclusions are based on the experimental data taken at the reduced frequency less than 0.03. Depending on the ambient conditions, three distinctively different flow characteristics were observed.

1. There was no observable unsteadyness effect when the foil was oscillated about a large mean angle of attack and small cavitation number so that a natural (non-ventilated) supercavity always existed. This is to be expected at the relatively low frequency range tested.

2. When a foil with a ventilated cavity was oscillated about a large mean angle of attack, the cavity pressure as well as the lift and drag also oscillated at the same frequency as that of the foil oscillation, but with a phase difference. The amplitudes of oscillation for the cavitation number and for the lift and drag coefficients are increasing functions of the air supply coefficient and decreasing functions of the reduced frequency. Nevertheless, it was found that the instantaneous lift and drag coefficients agreed with their steady flow counterparts based on the instantaneous angle of attack and the instantaneous cavitation number. The phase shift of the cavity pressure oscillation is a function of the reduced frequency. With a sufficient ventilation rate, two types of pressure pulsation, that of a pulsating cavity and that due to the angular oscillation, may co-exist.

3. Naturally cavitating flow at small angle of attack ($\alpha < 6^{\circ}$) for the flat plate was found to be very unstable. There existed two alternate cavity conditions for any given steady ambient condition. Consequently, force on the foil was also found to be unstable. For this reason, a rather erratic flow was observed when the foil was oscillated about a small mean angle of attack at small cavitation number. Furthermore, the instantaneous lift coefficient at any instantaneous angle of attack was considerably lower than the corresponding steady flow value.

B. Sudden Ventilation

When air was suddenly supplied to an otherwise non-ventilated cavity, both the cavity pressure and the cavity length increased with time whereas

the lift force decreased with time. The change in cavity length and lift force appeared to lag behind the cavity pressure change. The rate of increase of the cavity length increased with the air supply rate, but never exceeded the free-stream speed.

C. Sudden Angle of Attack Change

The response of the lift coefficient to a zero order unit step function change in the angle of attack was estimated using the experimental data for a nearly constant rate of angle change. To avoid the natural frequency of the system, the numerical differentiation of the lift data had to be performed using an interval not less than 0.05 second. Moreover, the period of the cavity length vibration was of the order of 0.1 second, which was small enough to interfere with the response function. The response time of the system due to angle of attack change was apparently less than 0.1 second and, hence, a faster rotation ($T < 0.1$ sec) is necessary for a better result.

The present report on pitching oscillations is limited to a very low reduced frequency range. A new program concerned with a considerably higher frequency range is now in progress and a report of the result will follow at a later date.

LIST OF REFERENCES

[1] Song, C. S. and Silberman, E. Experimental Studies of Cavitation Noise in a Free-Jet Tunnel, University of Minnesota, St. Anthony Falls Hydraulic Laboratory, Technical Paper No. 33, Series B, July 1961.

[2] Silberman, E. and Ripken, J. F. The St. Anthony Falls Hydraulic Laboratory Gravity-Flow Free-Jet Water Tunnel, University of Minnesota, St. Anthony Falls Hydraulic Laboratory, Technical Paper No. 24, Series B, August 1959.

[3] Silberman, E. and Daugherty, R. H. A Dynamometer for the Two-Dimensional, Free-Jet Water Tunnel Test Section, University of Minnesota, St. Anthony Falls Hydraulic Laboratory, Technical Paper No. 40, Series B, June 1962.

[4] Silberman, E. "Experimental Studies of Supercavitating Flow about Simple Two-Dimensional Bodies in a Jet," Journal of Fluid Mechanics, Vol. 5, Part 3, 1959.

[5] Wade, R. B. Water Tunnel Observations on the Flow Past a Plane-Convex Hydrofoil, California Institute of Technology Report No. E-79-6, February 1964.

[6] Parkin, Blaine R. Experiments on Circular Arc and Flat Plate Hydrofoils in Non-Cavitating and Full Cavity Flows, California Institute of Technology, Hydrodynamic Laboratory, Report No. 47-6, February 1956.

[7] Silberman, E. and Song, C. S. "Instability of Ventilated Cavities," Journal of Ship Research, Vol. 5, No. 1, June 1961.

[8] Song, C. S. "Pulsation of Two-Dimensional Cavities," Fourth Symposium on Naval Hydrodynamics, Washington, D. C., August 1962.

[9] Lamb, H. Hydrodynamics, Sixth Edition, Dover Press: April, 1945

F I G U R E S

(1 through 31)

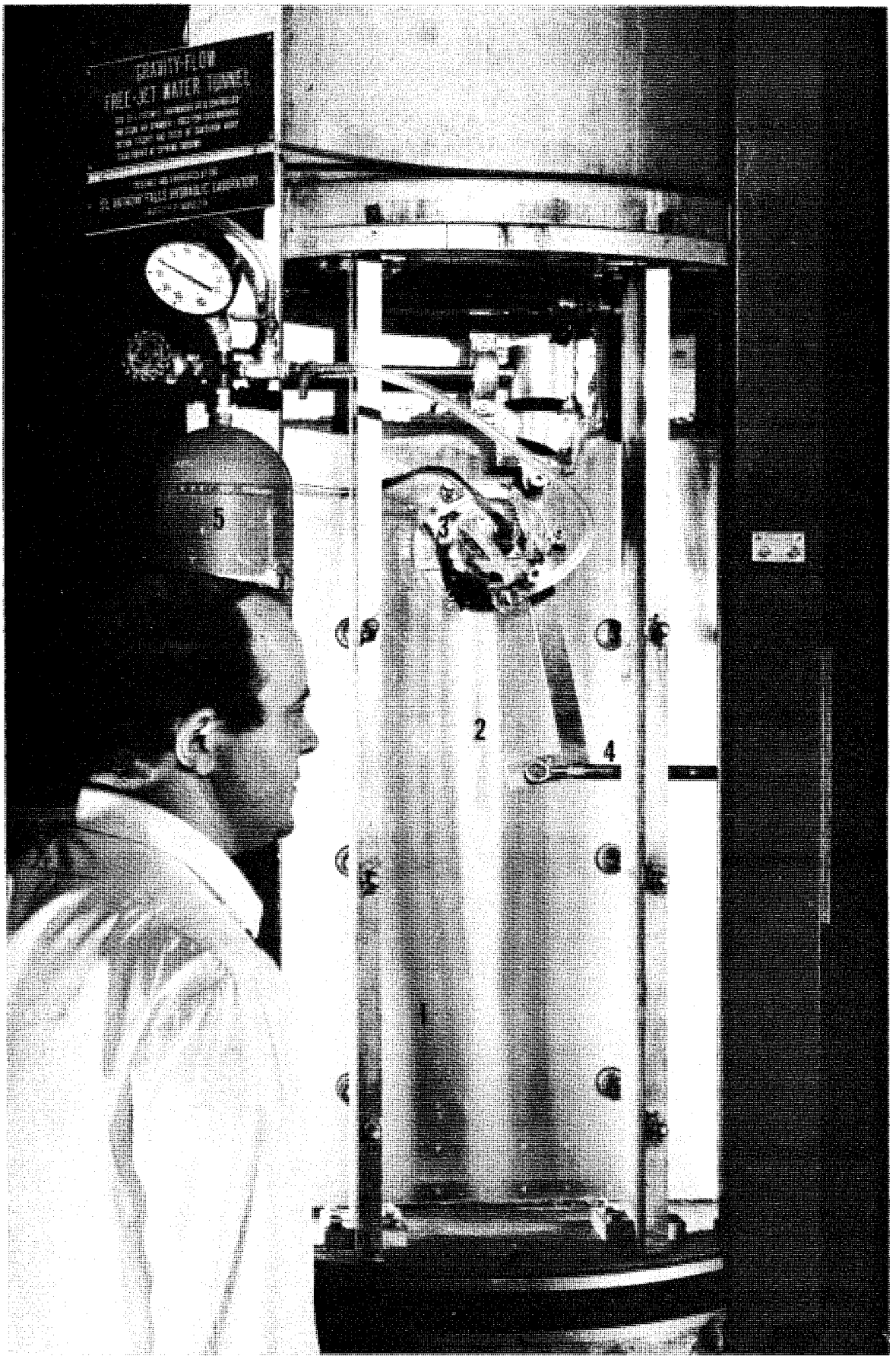

Fig. 1 - A view of the free-jet tunnel with foil and dynamometer (1 = free-jet; 2 = cavity; 3 - dynamometer; 4 = driving rod; 5 = air tank)

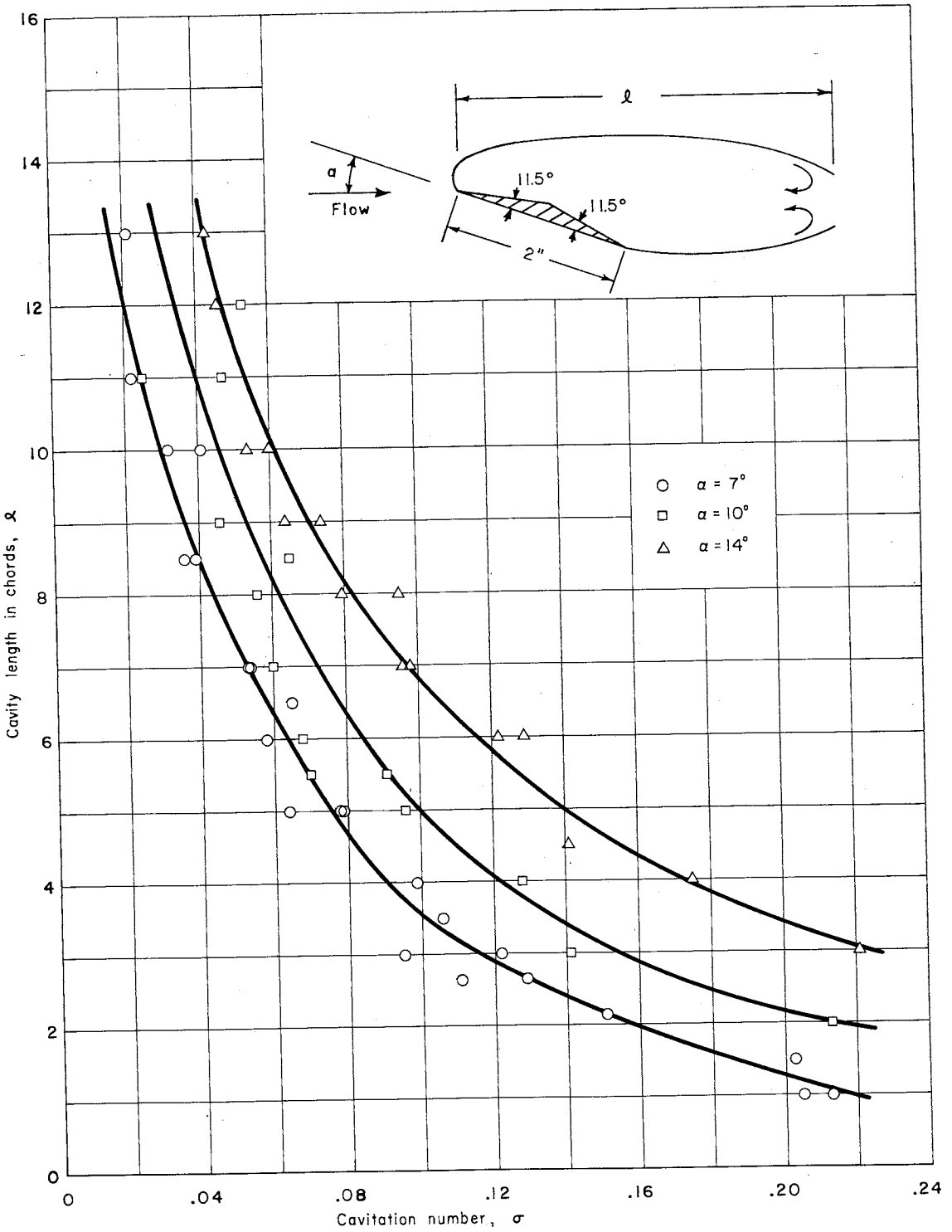

Fig. 2 - Steady flow cavity length for a flat plate hydrofoil

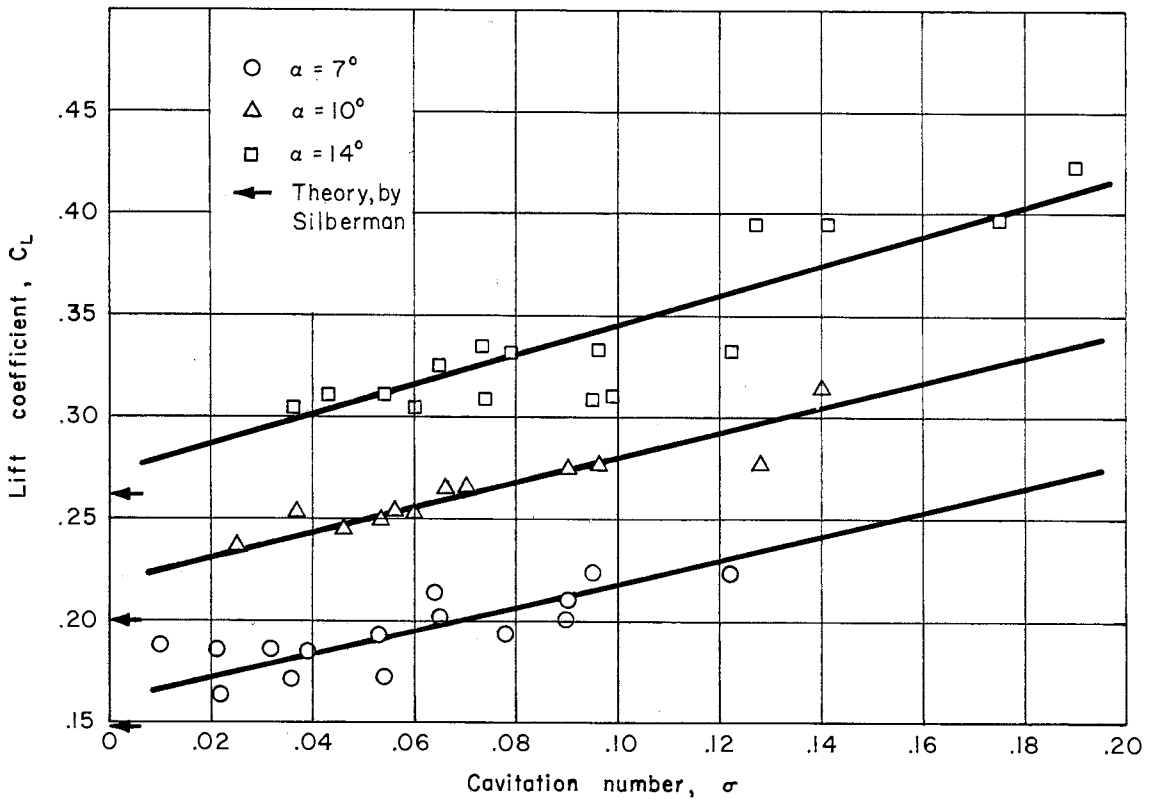

(a) Lift coefficient

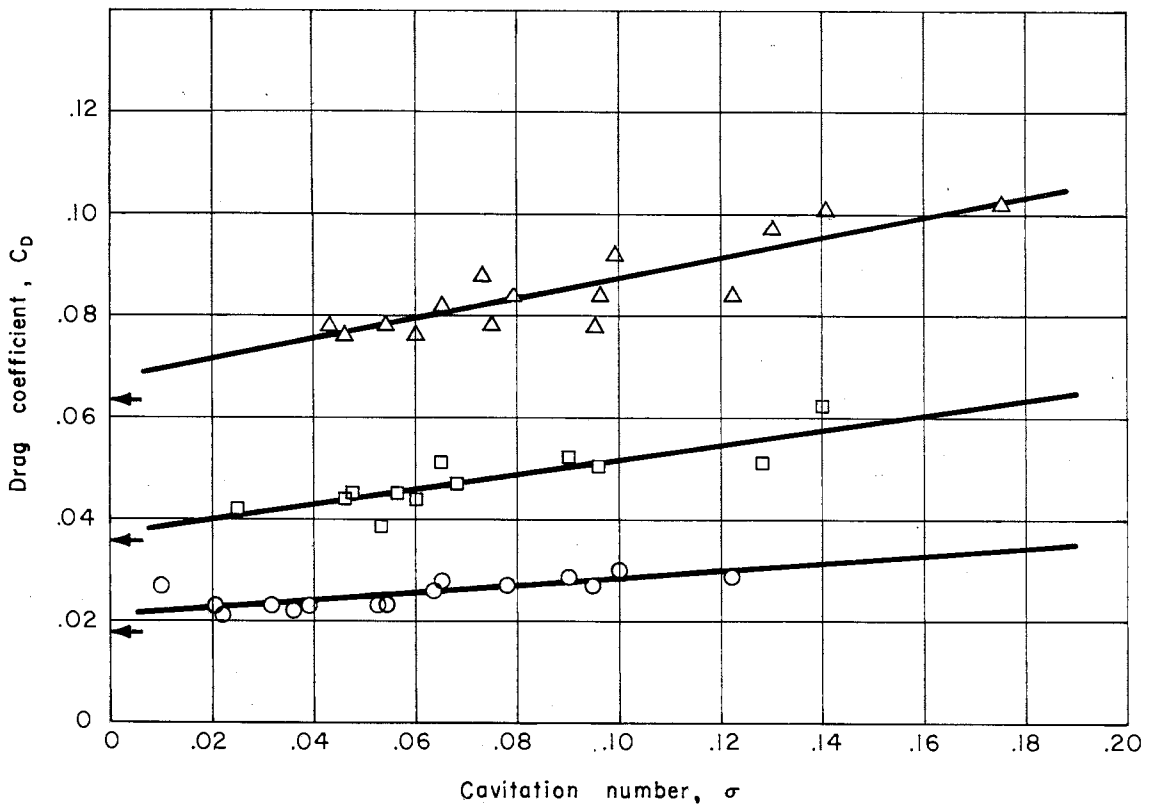

(b) Drag coefficient

Fig. 3 - Steady flow lift and drag coefficients, flat plate with supercavity

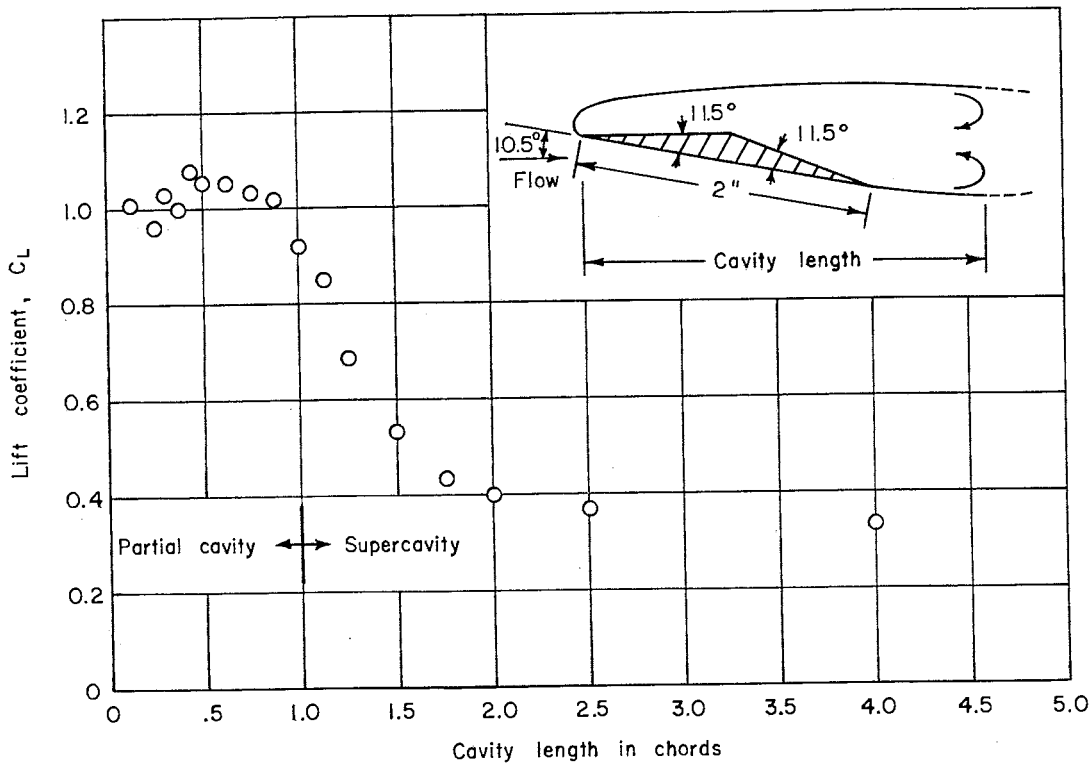

(a) Lift coefficient

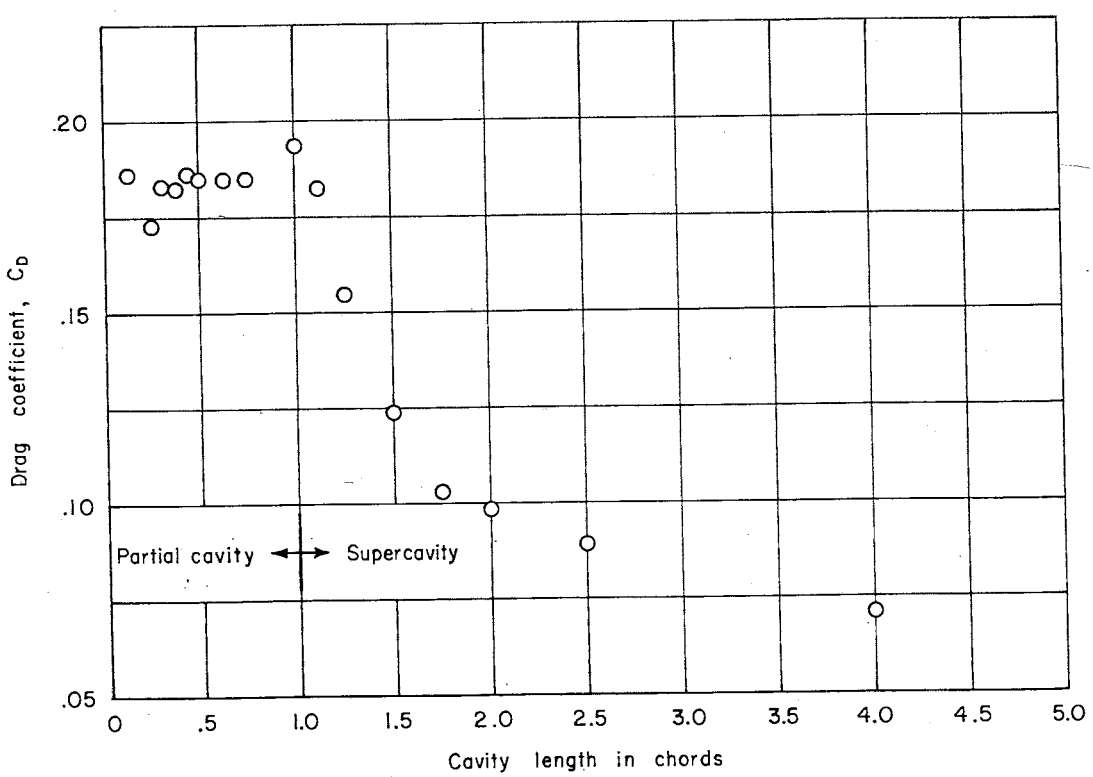

(b) Drag coefficient

Fig. 4 - Steady flow lift and drag coefficients, flat plate with and without cavity

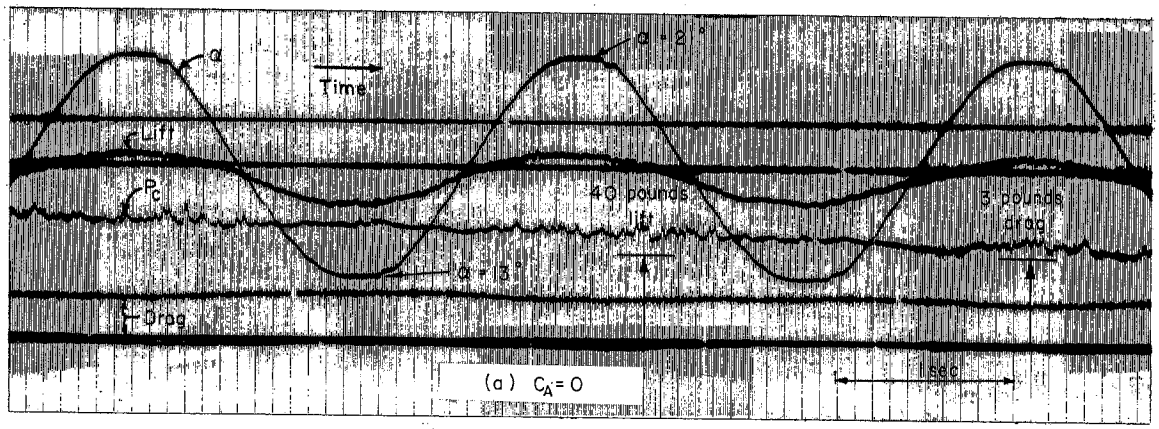

V = 44.0 fps k = 0.005 σ = 0.118
ℓ = 6" ~ 10" α = 13° ~ 21°

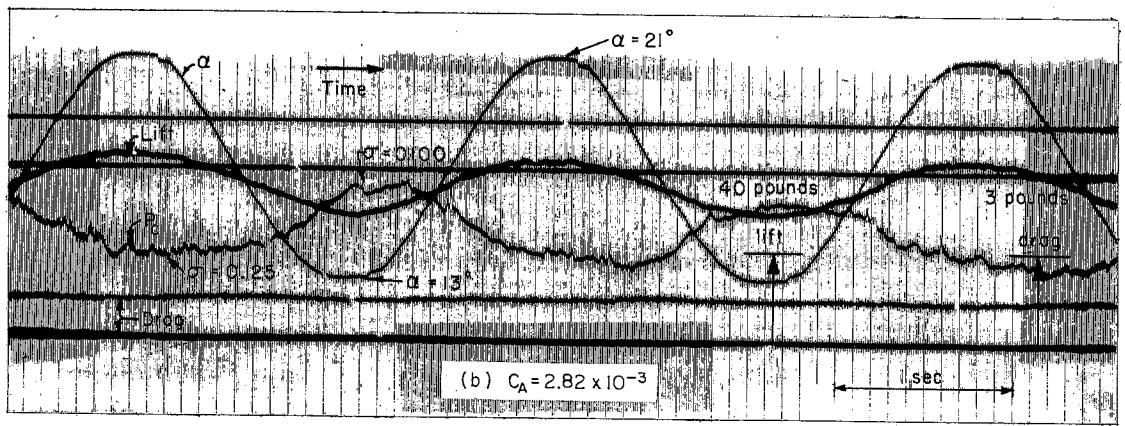

V = 43.2 fps k = 0.005 σ = 0.100 ~ 0.125
ℓ = 11" ~ 13" α = 13° ~ 21°

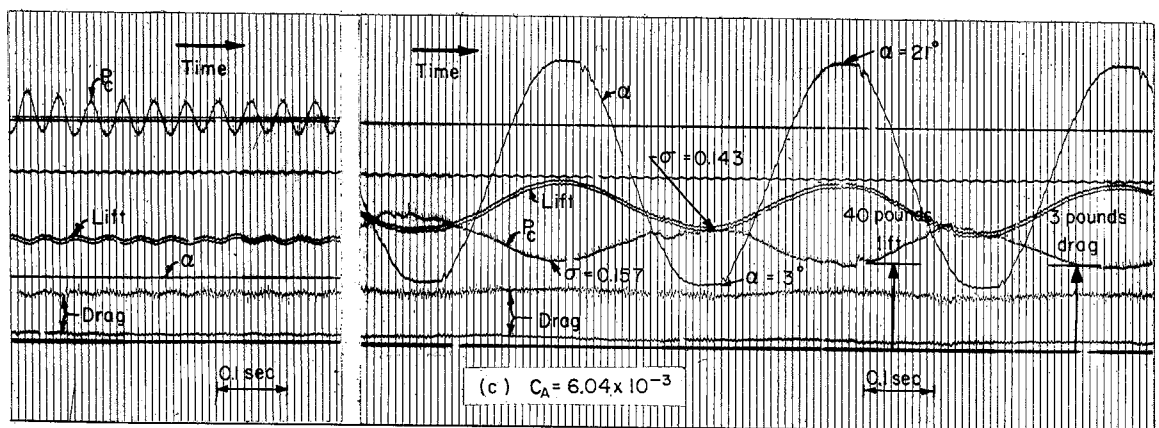

V = 42.7 fps k = 0 σ = 0.053
α = 13°

V = 42.7 fps k = 0.031 σ = 0.143 ~ 0.157
ℓ = 11" ~ 13" α = 13° ~ 21°

Fig. 5 - Typical data for an oscillating plate

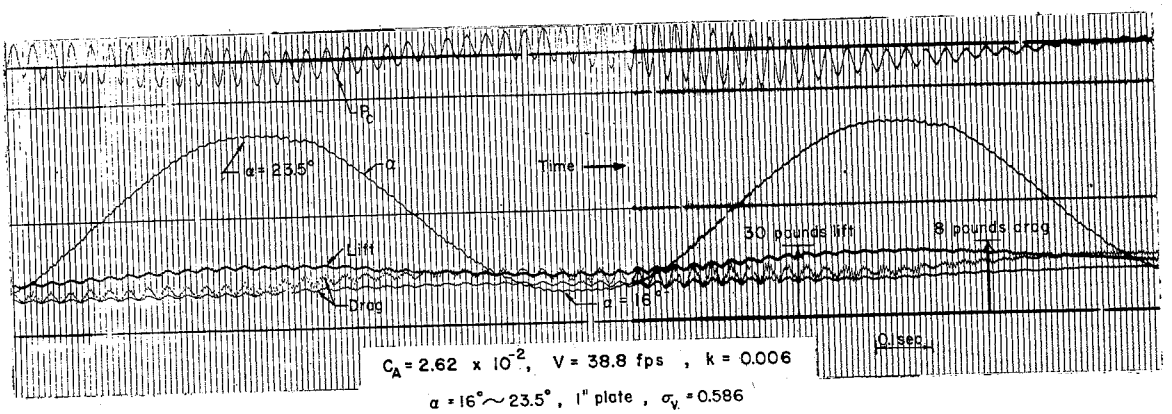

Fig. 6 - Record of pulsating cavity behind an oscillating plate

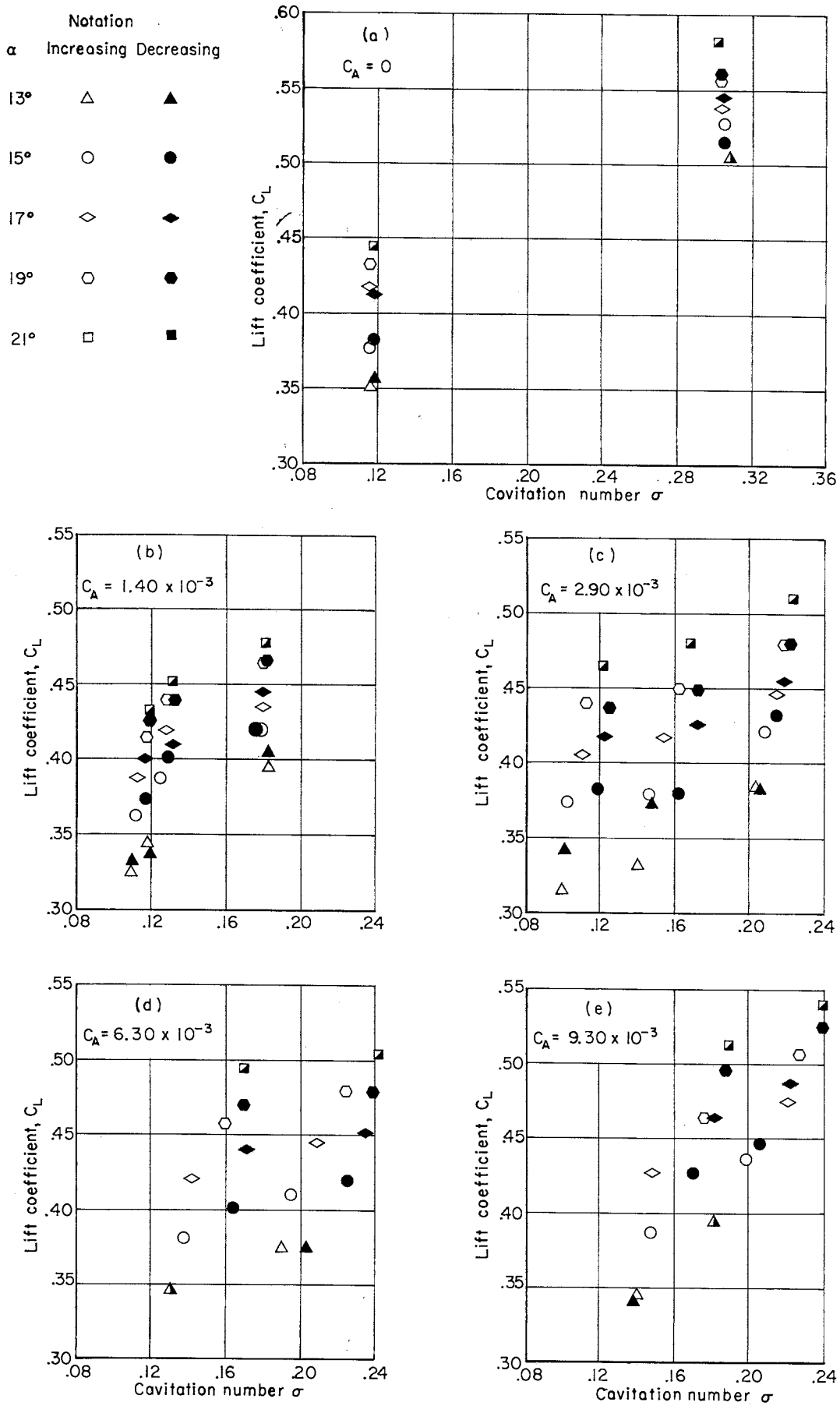

Fig. 7 – Effect of ventilation on instantaneous lift coefficient (k = 0.0055)

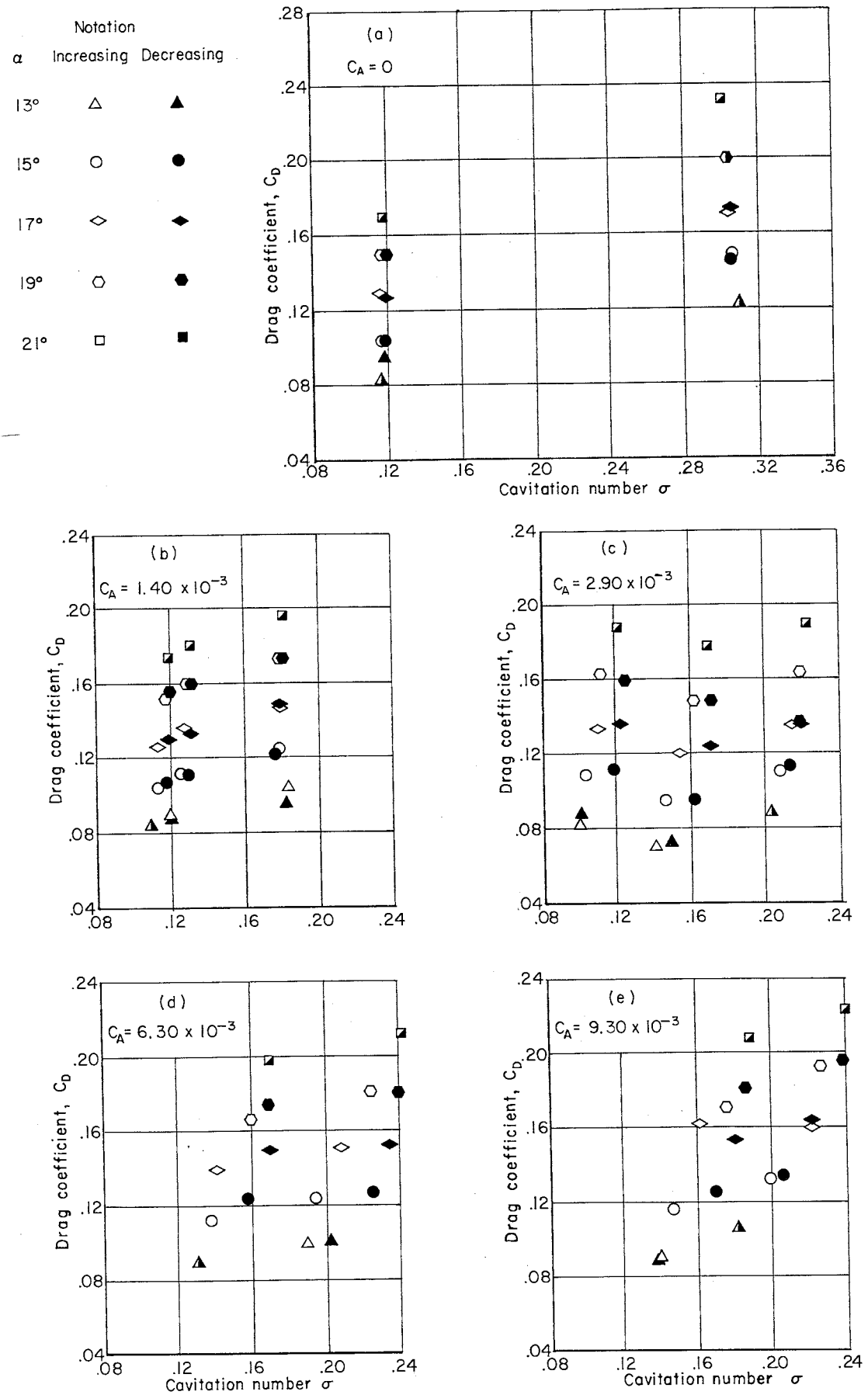

Fig. 8 – Effect of ventilation on instantaneous drag coefficient (k = 0.0055)

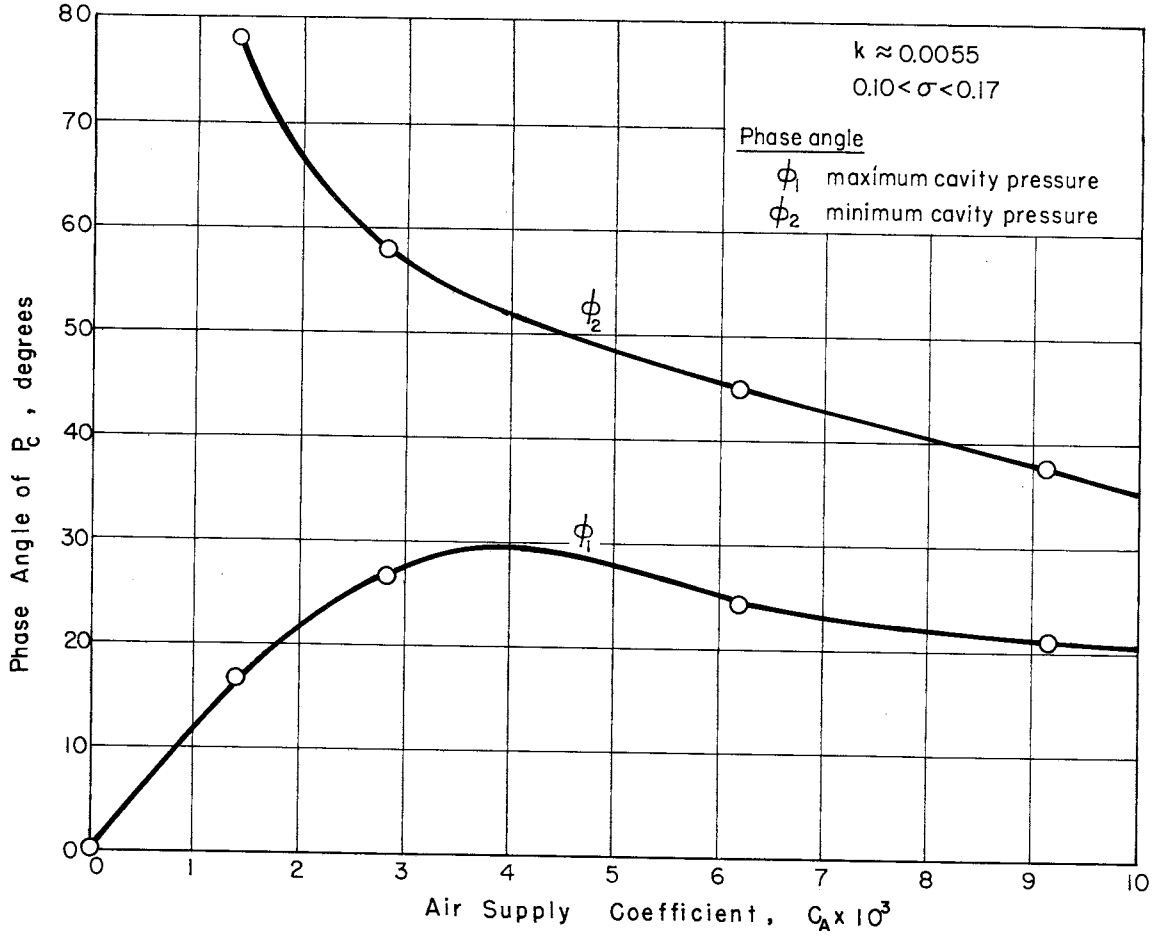

Fig. 9 - Phase angle of cavity pressure oscillation

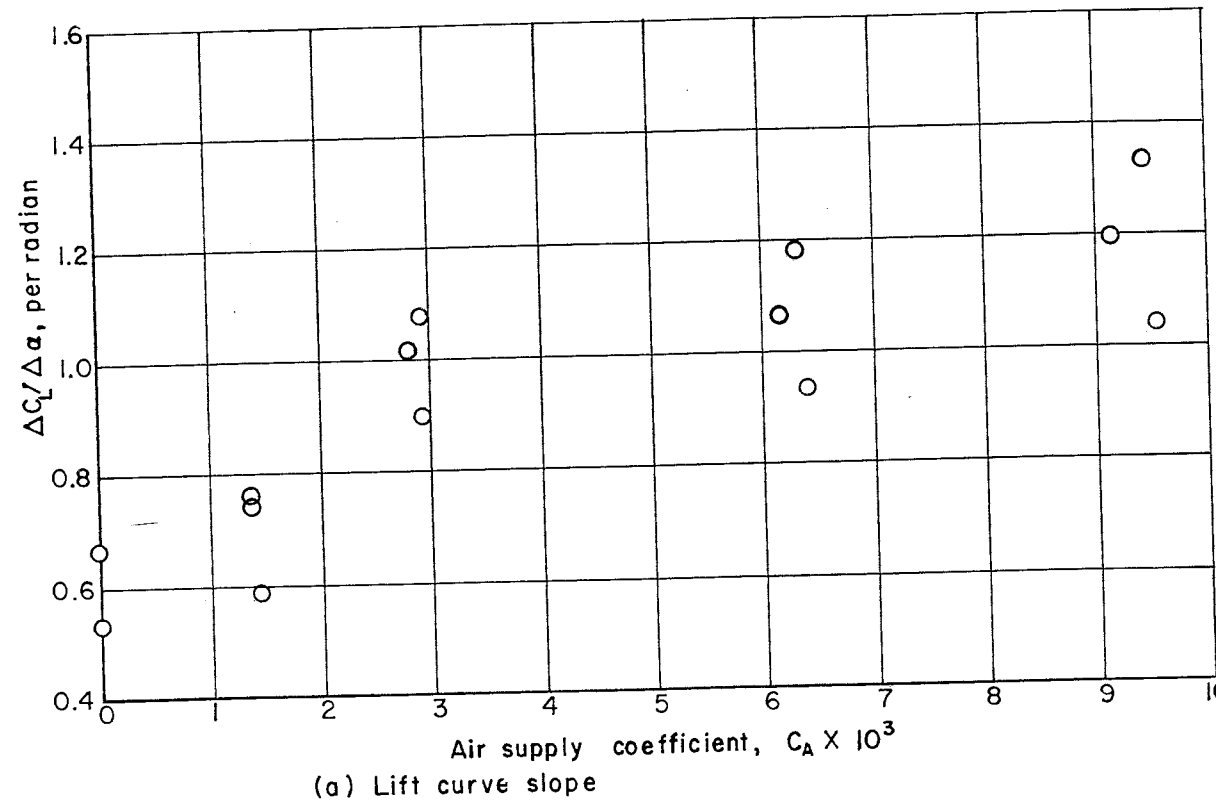

(a) Lift curve slope

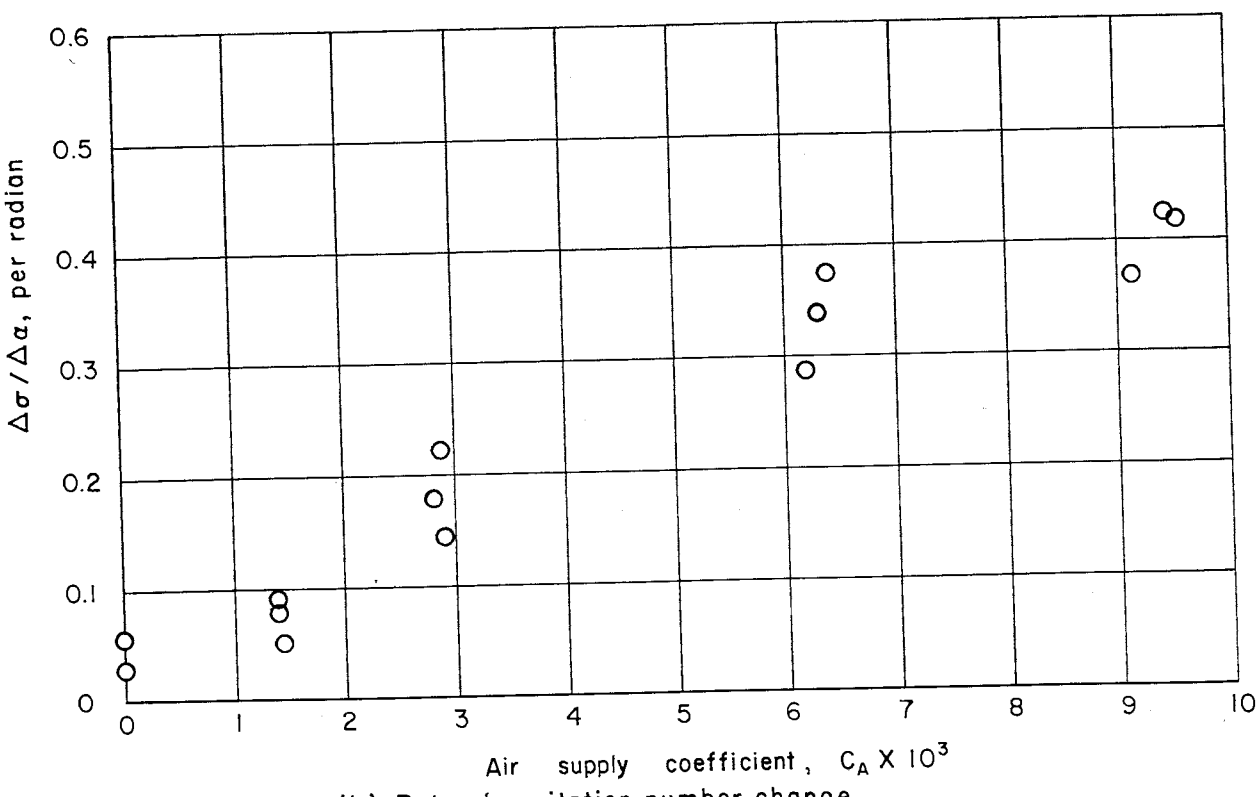

(b) Rate of cavitation number change

Fig. 10 - Effect of ventilation on lift curve slope and cavitation number change during oscillation (k = 0.0055)

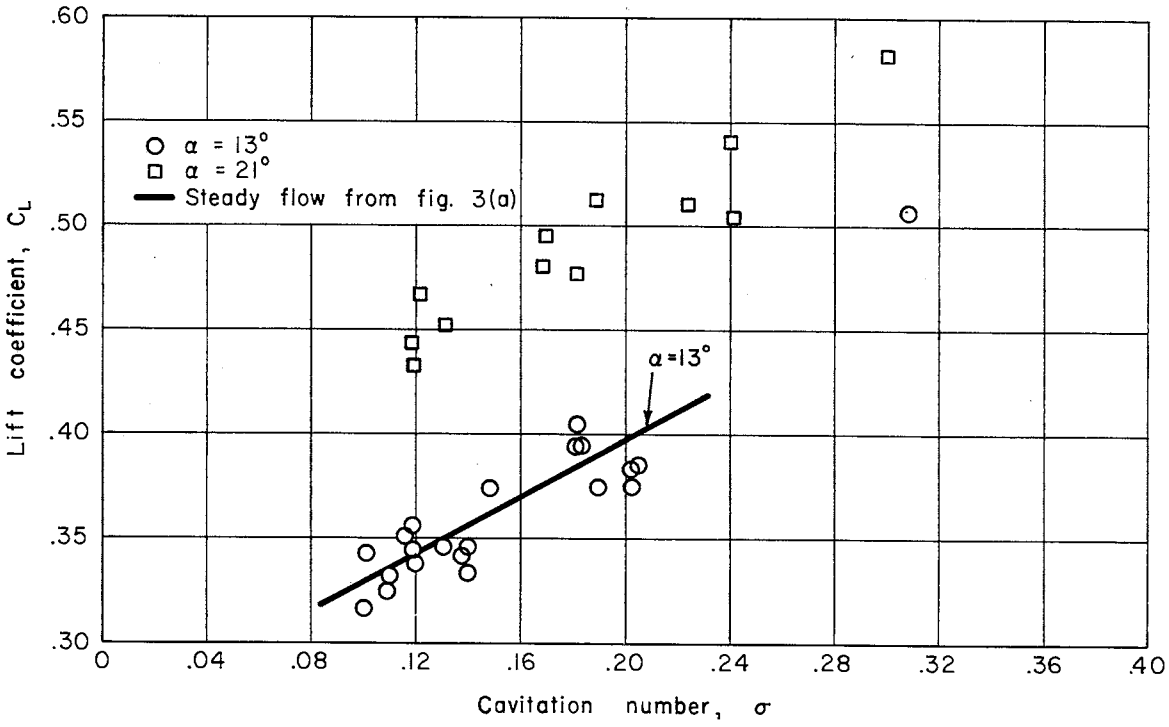

Fig. 11 - Lift coefficient as a function of instantaneous angle of attack and instantaneous cavitation number (k = 0.0055)

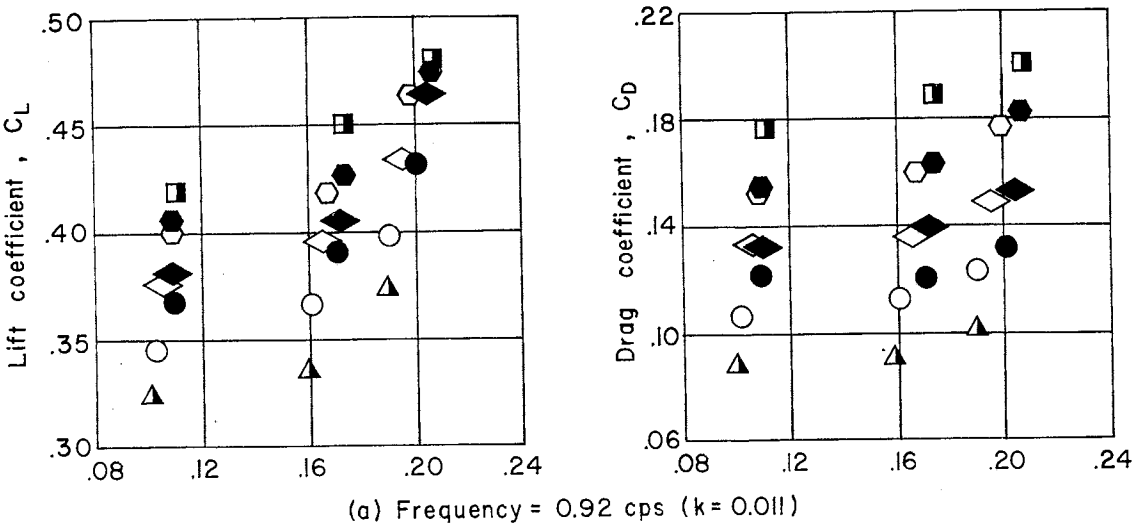

(a) Frequency = 0.92 cps (k = 0.011)

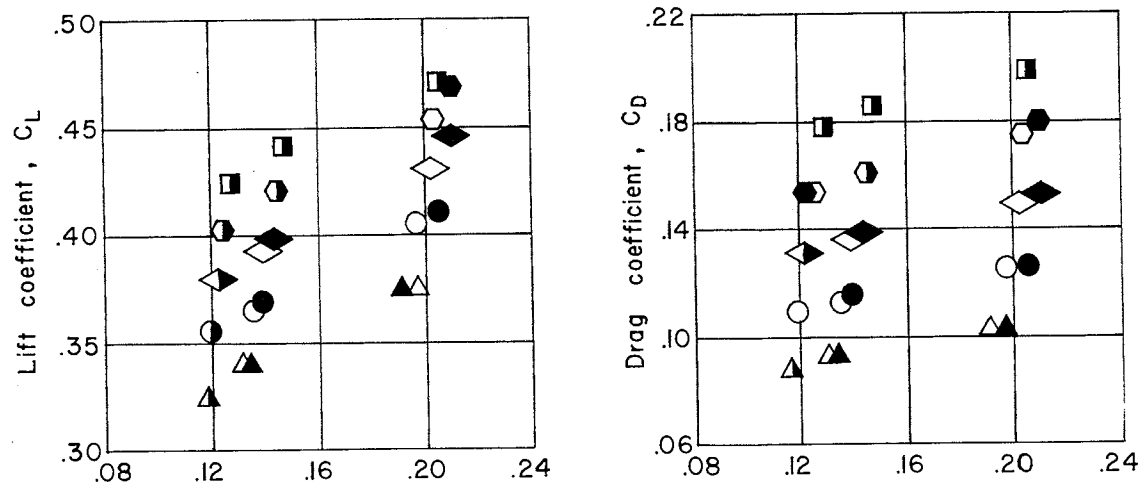

(b) Frequency = 2.08 cps (k = 0.026)

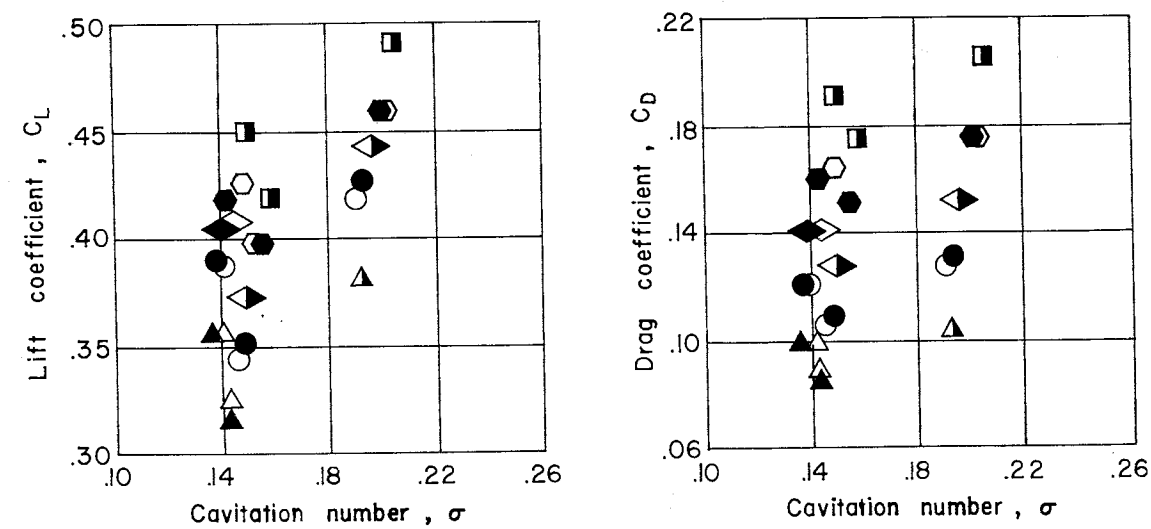

(c) Frequency = 2.56 cps (k = 0.032)

Fig. 12 - Instantaneous lift and drag coefficients as influenced by reduced frequency ($C_A = 6.3 \times 10^{-3}$, symbols as in Fig. 8)

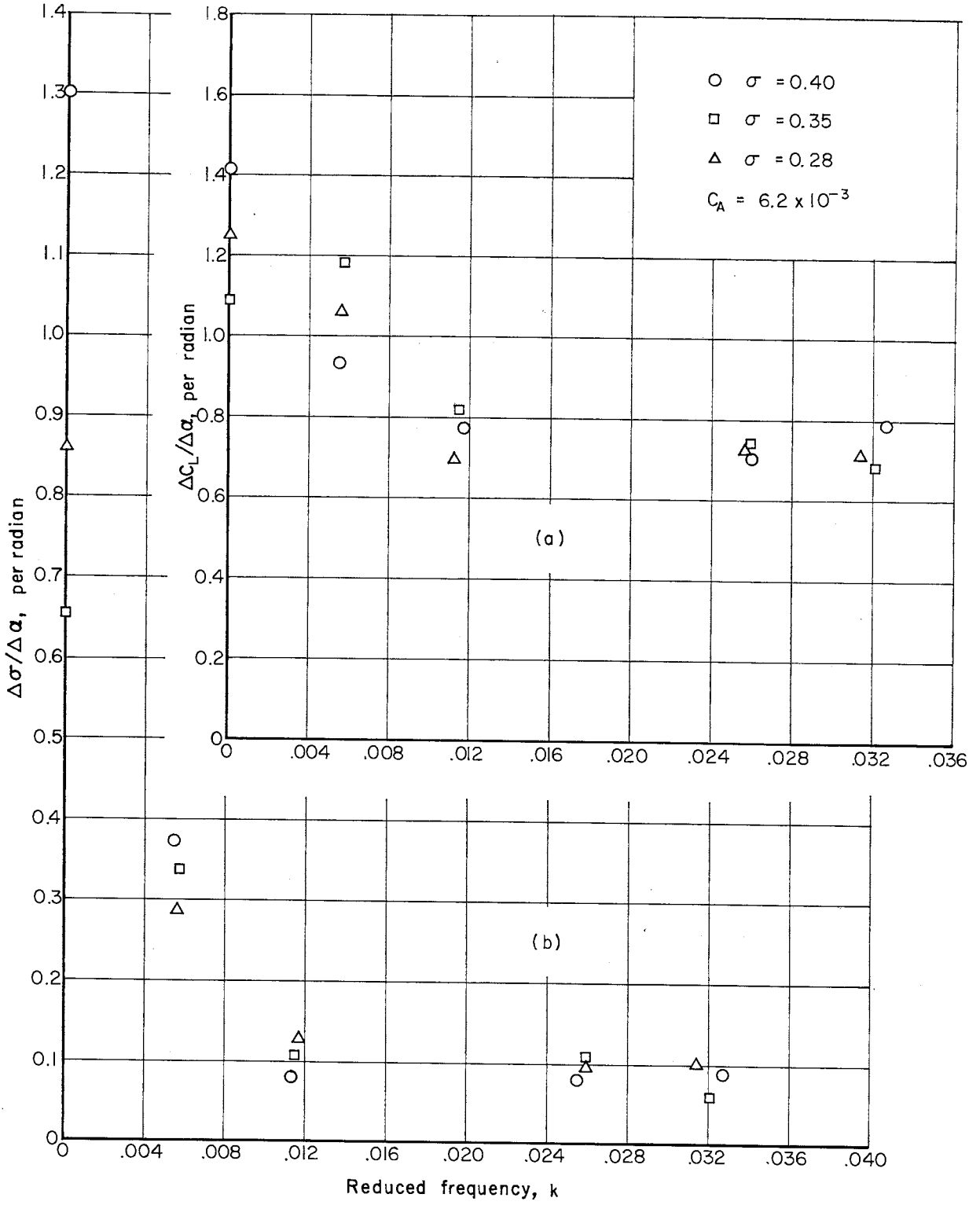

Fig. 13 - Effect of frequency on lift curve slope and rate of cavitation number change

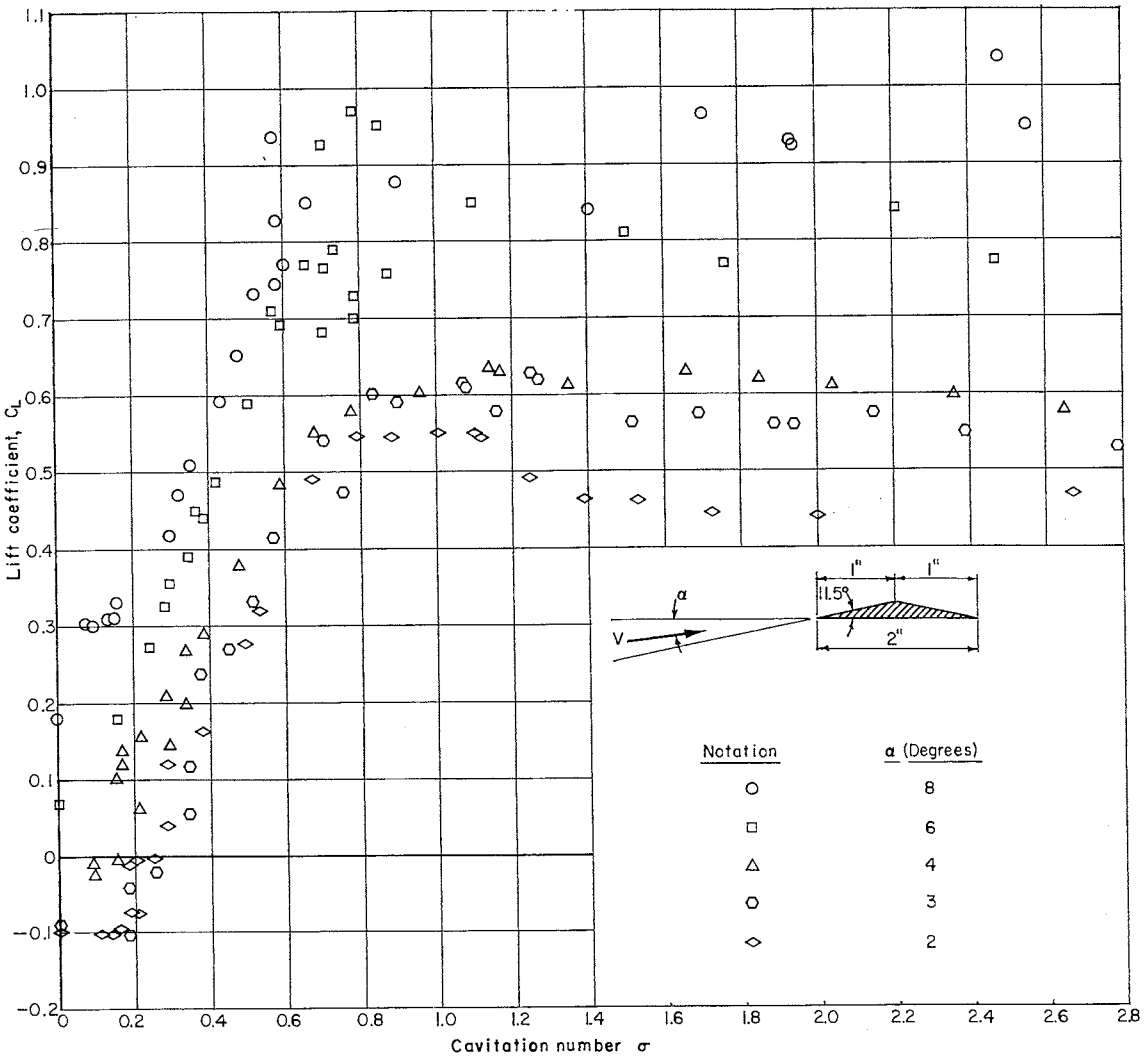

Fig. 14 - Steady state lift coefficients at small angle of attack for a flat plate hydrofoil

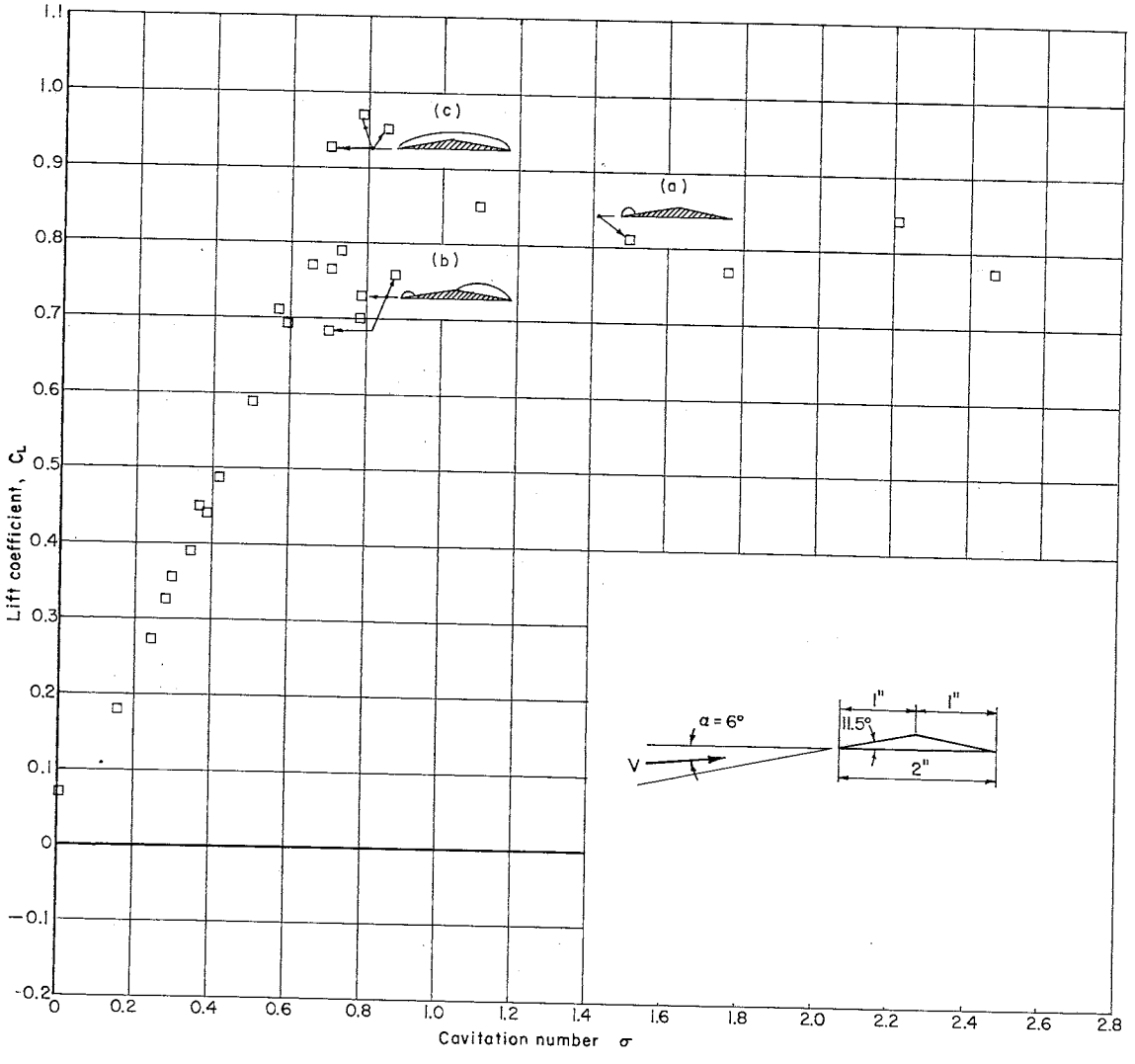

Fig. 15 - Steady lift coefficient and schematic cavity configuration for $\alpha = 6°$

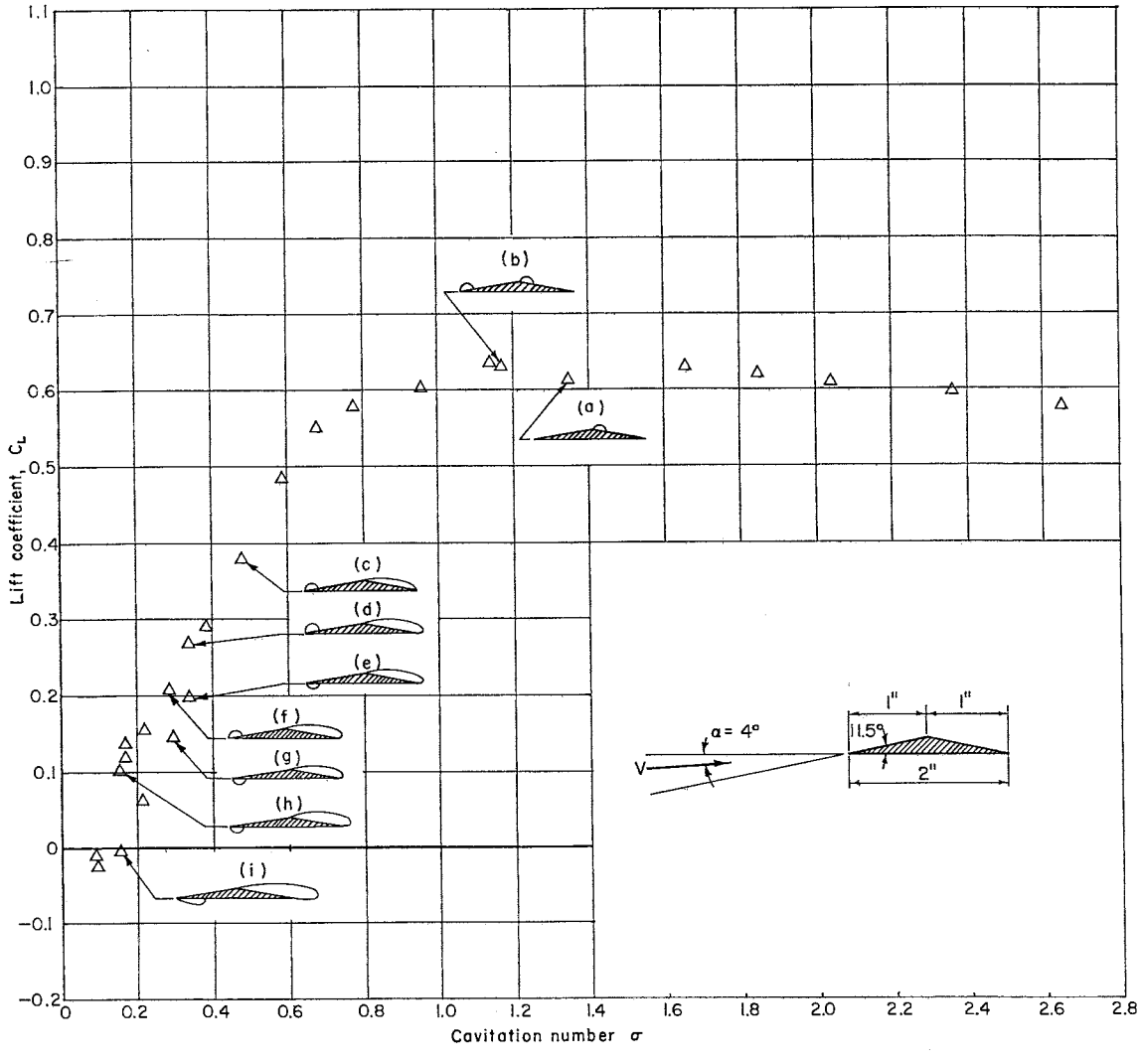

Fig. 16 - Steady lift coefficient and schematic cavity configuration for $\alpha = 4^{\circ}$

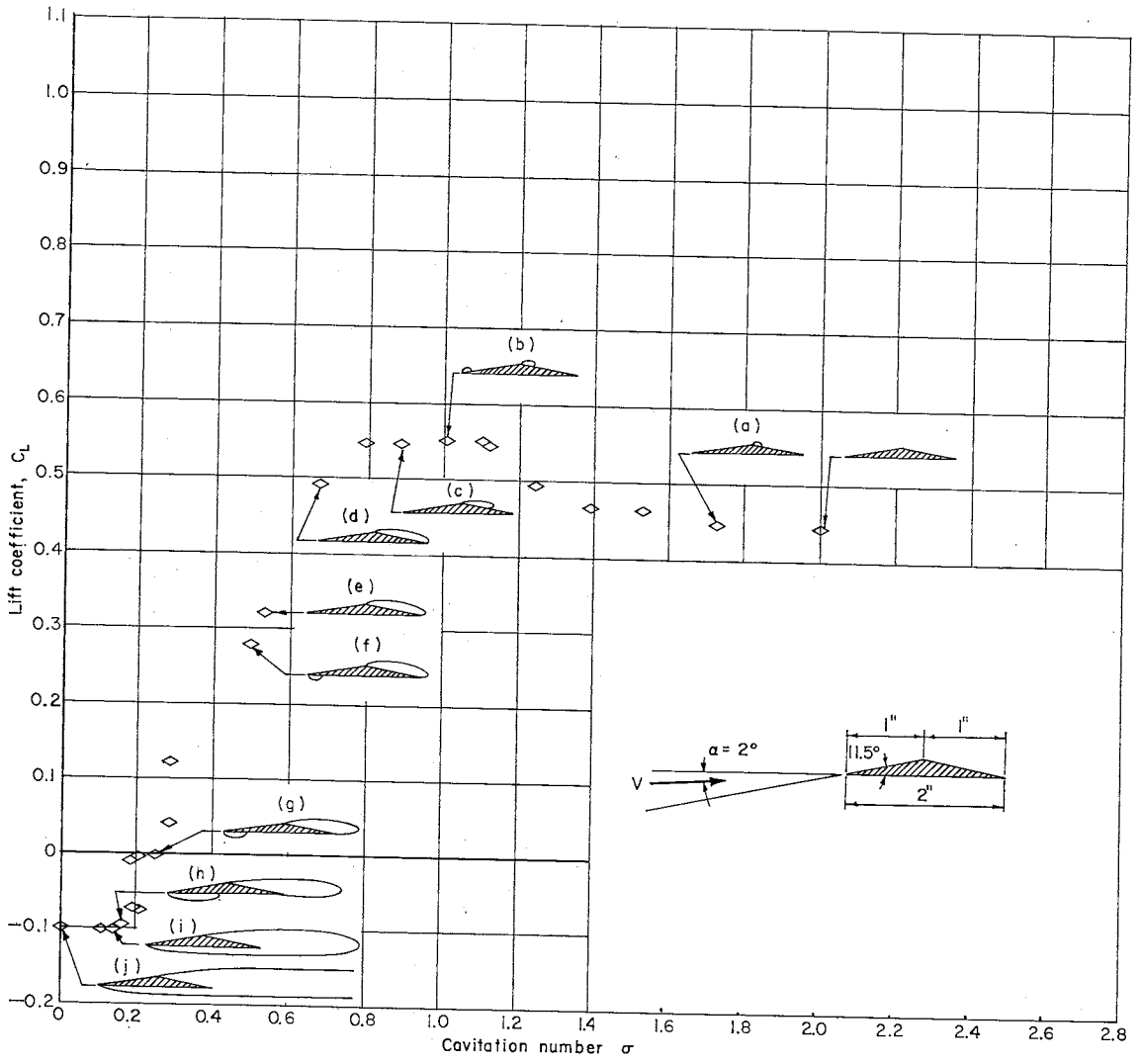

Fig. 17 - Steady lift coefficient and schematic cavity configuration for $\alpha = 2^{\circ}$

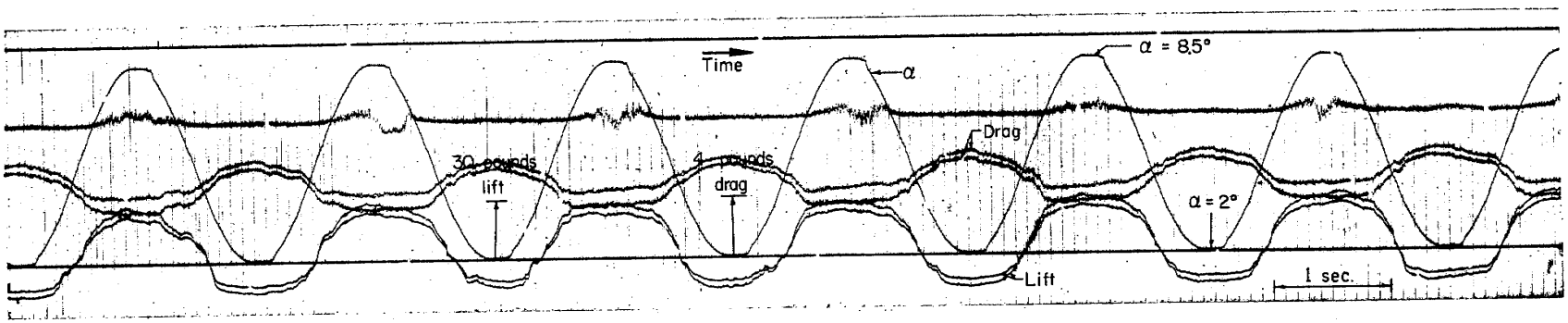

$\sigma_V = 0.163$, $k = 0.0119$, $C_A = 0$
$2° \leq \alpha \leq 8.5°$

Fig. 18 – Typical oscillographic record for oscillation about small mean angle of attack

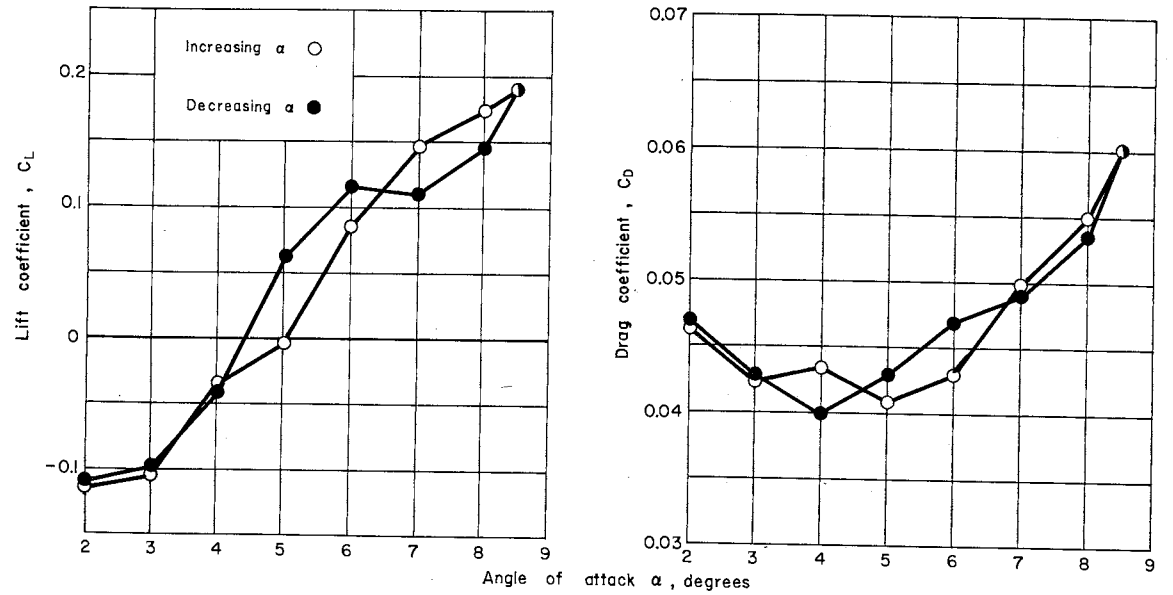

(a) $\sigma_v = 0.163$, $k = 0.0119$, $C_A = 0$

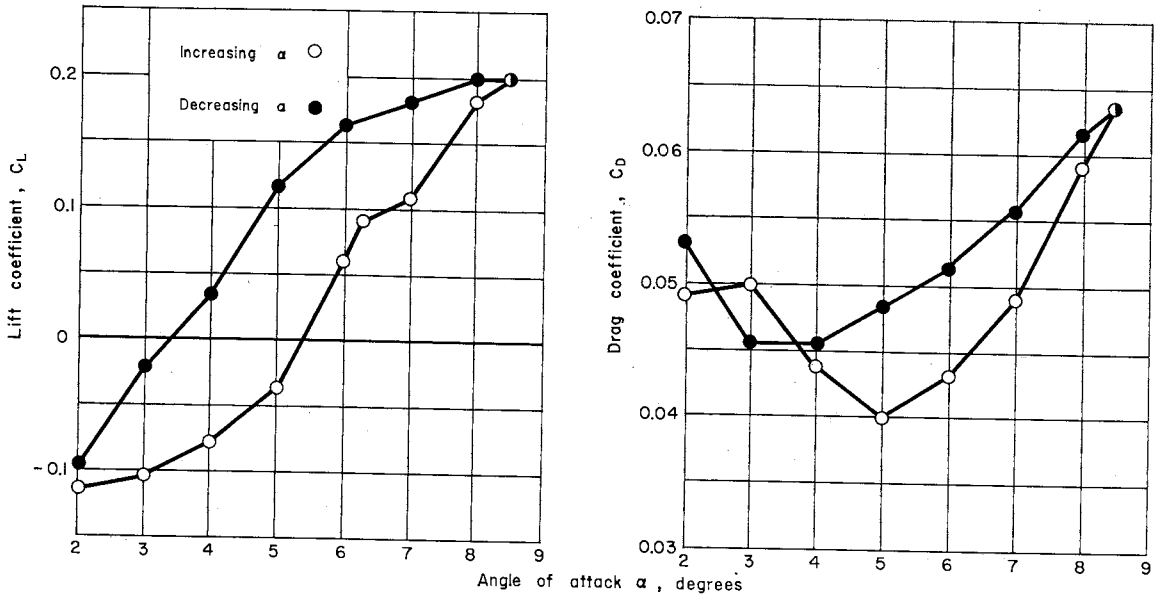

(b) $\sigma_v = 0.163$, $k = 0.0119$, $C_A = 0$

Fig. 19 - Instantaneous lift and drag coefficients at small angle of attack and small cavitation number

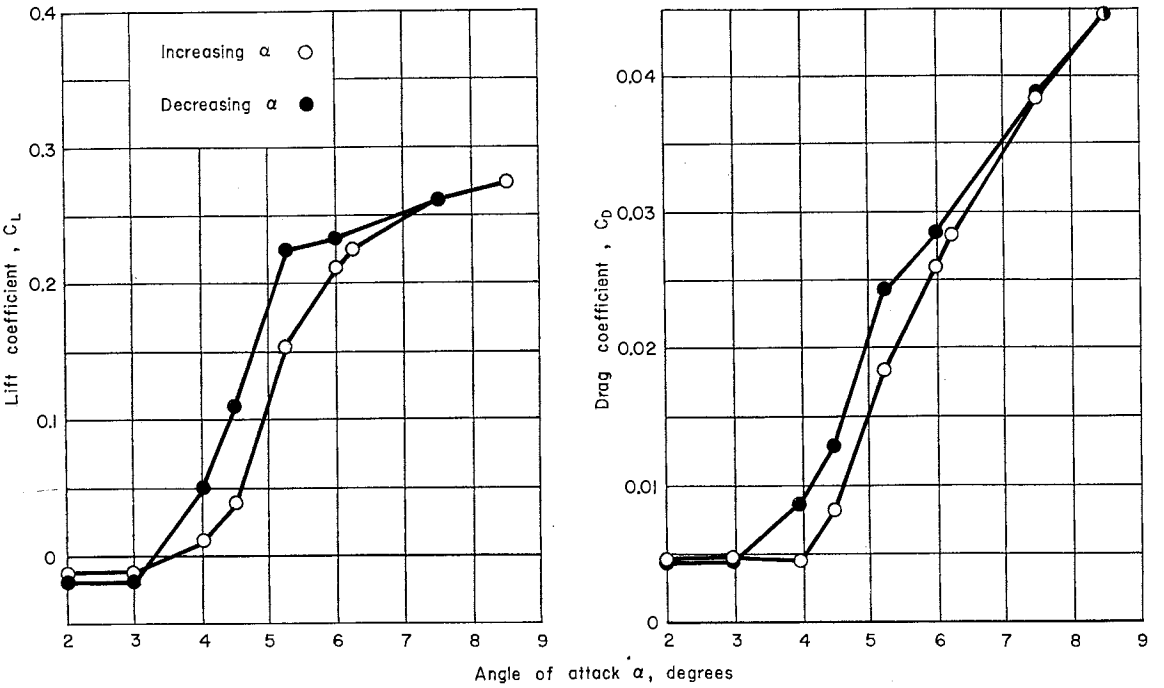

(a) $\sigma_v = 0.272$, $k = 0.0014$, $C_A = 0$

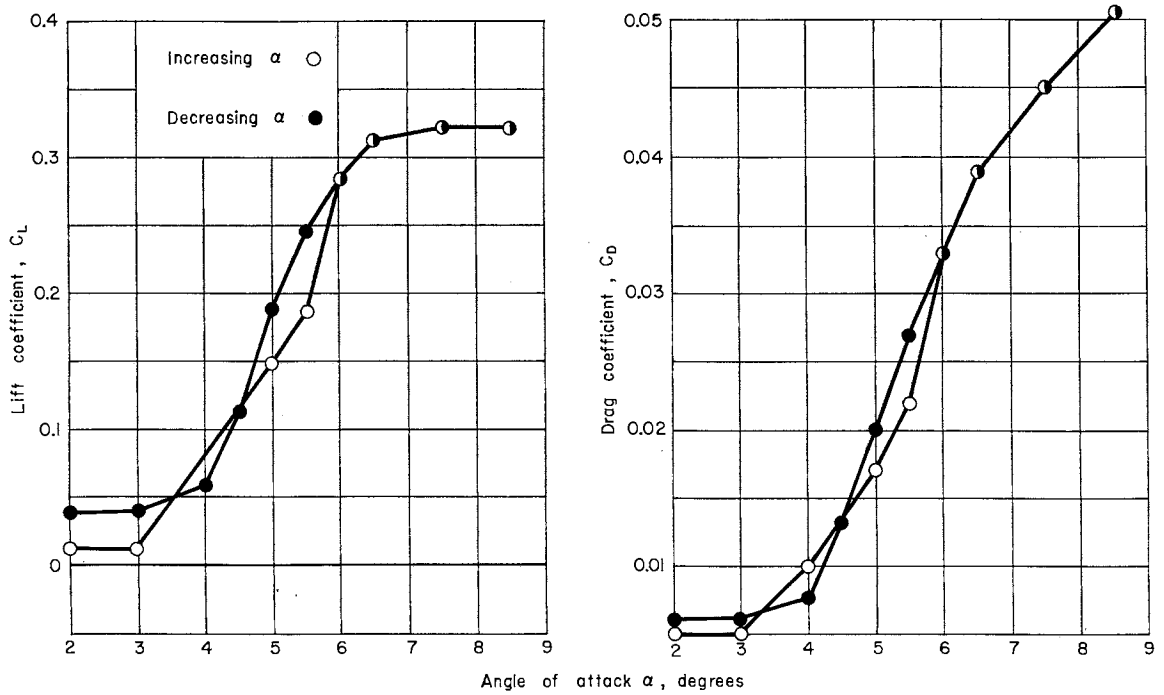

(b) $\sigma_v = 0.316$, $k = 0.0015$, $C_A = 0$

Fig. 20 - Instantaneous lift and drag coefficients at small angle of attack and moderately small cavitation number

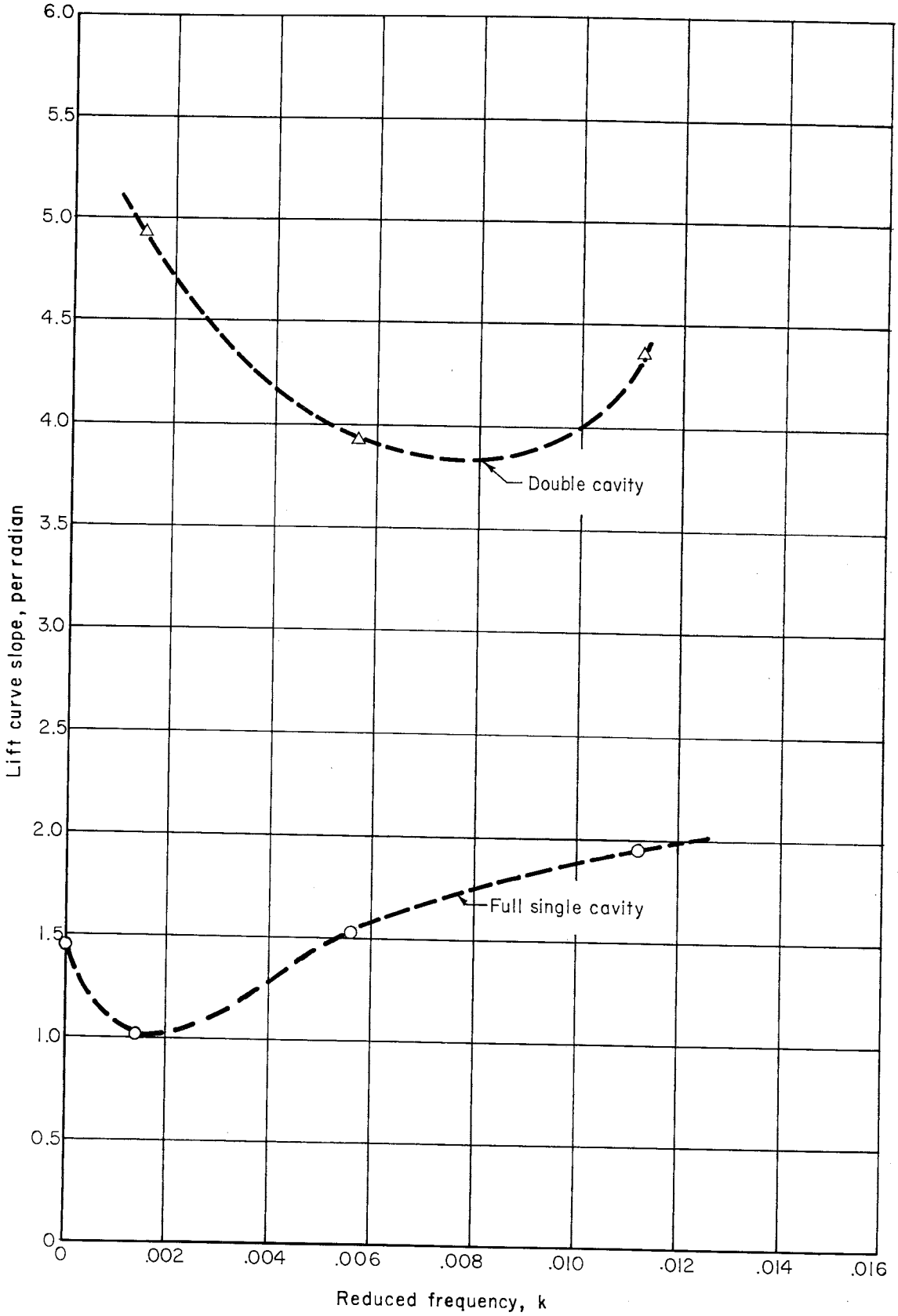

Fig. 21 - Frequency effect on lift curve slope for two flow regimes

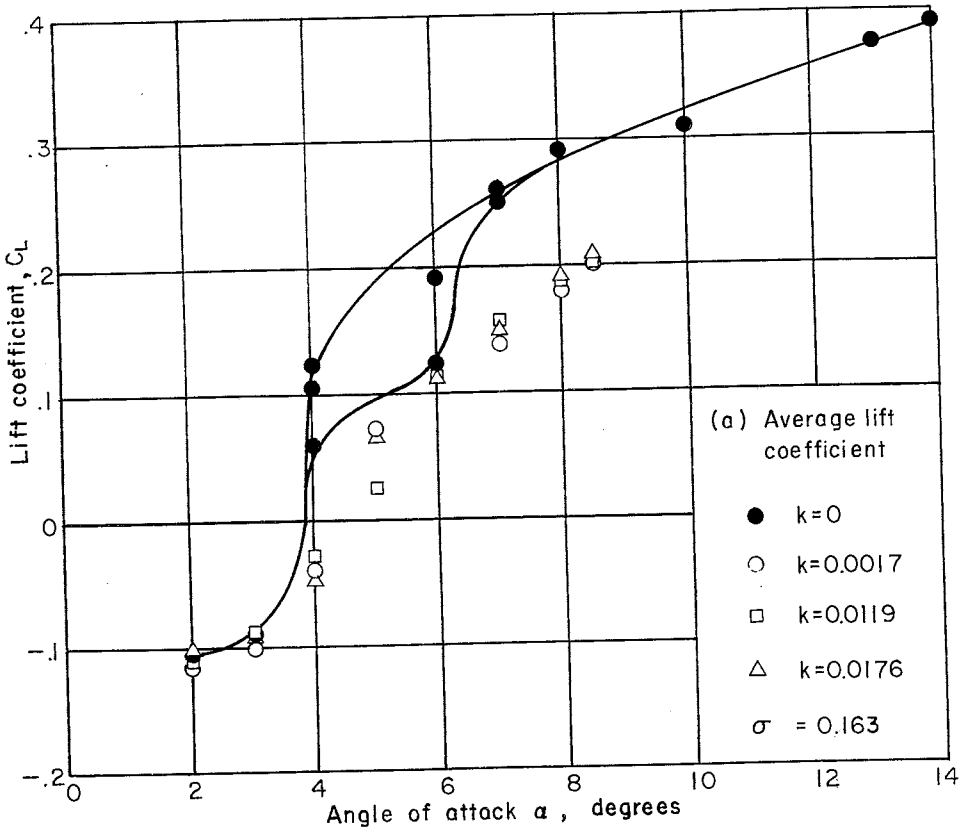

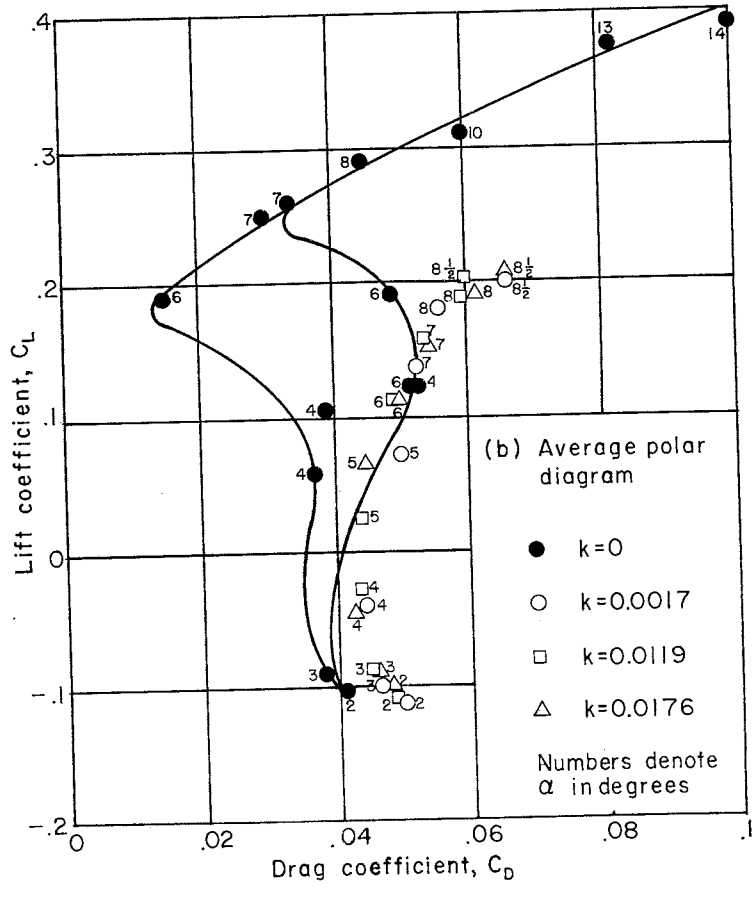

Fig. 22 - Comparison of forces on steady foil and oscillating foil at small angle of attack

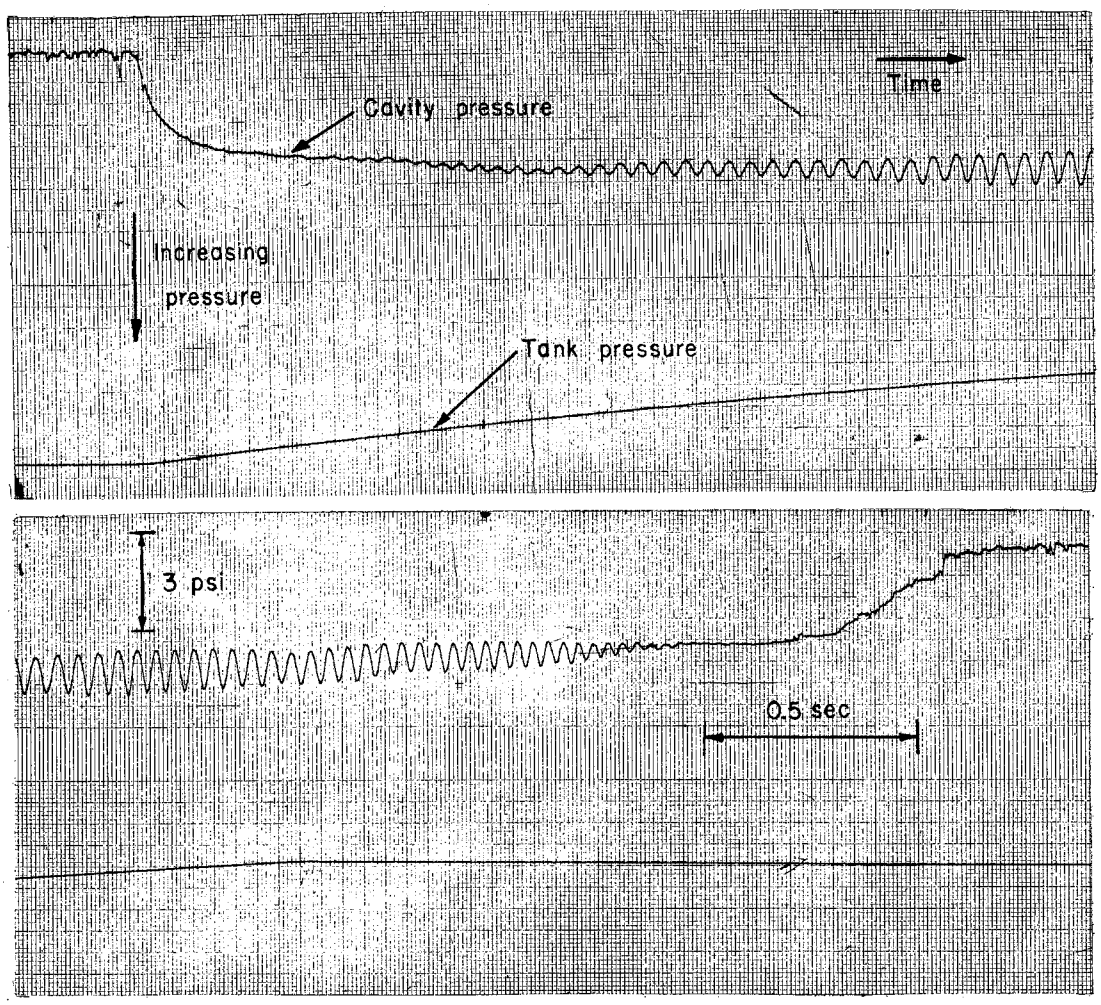

(a) Pulsating cavity , $\frac{3}{16}$" normal plate , $\sigma_v = 0.40$

Initial tank pressure = 22.82 psia

Rate of air tank pressure decrease = 4.88 psi / sec

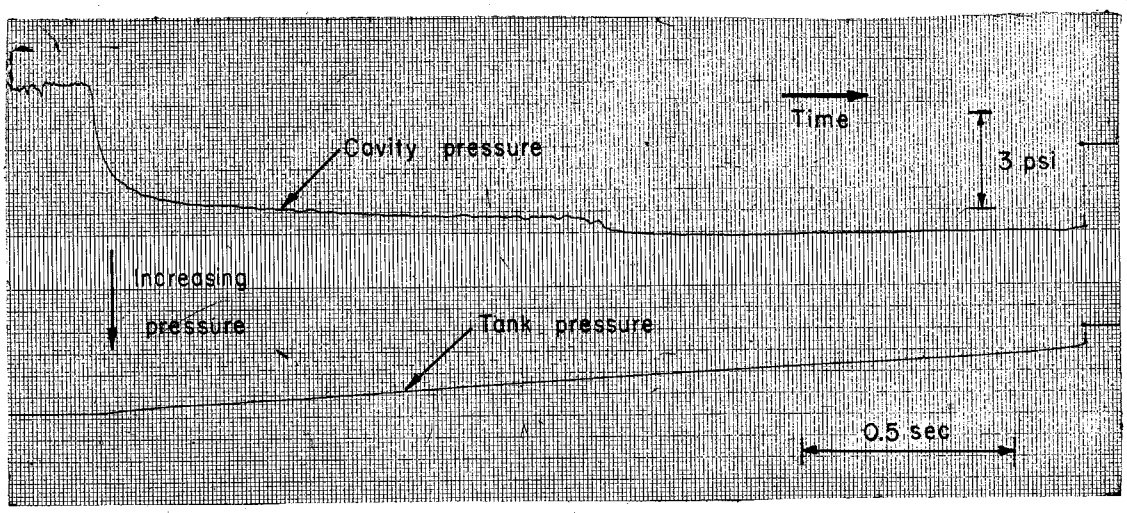

(b) Split cavity , $\frac{3}{16}$" normal plate , $\sigma_v = 0.40$

Initial tank pressure = 23.75 psia

Rate of air tank pressure decrease = 7.61 psi / sec

Fig. 23 - Typical records of air tank pressure and cavity pressure for sudden ventilation, normal plate

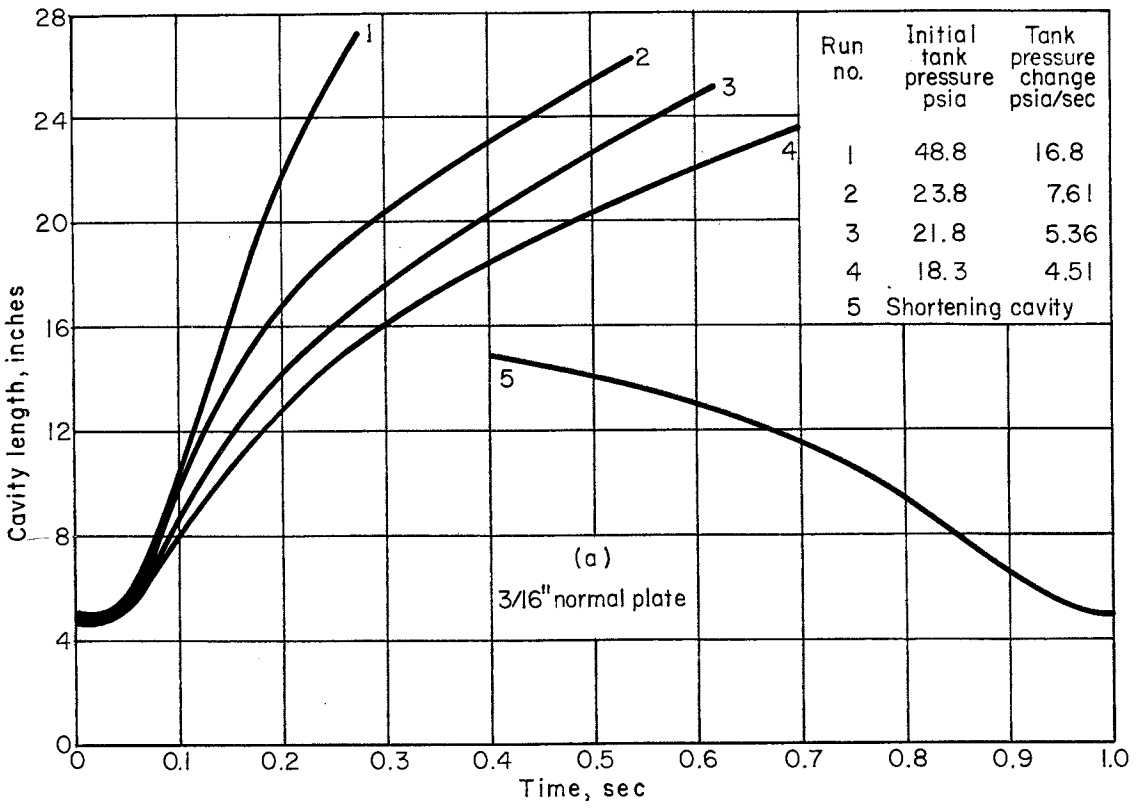

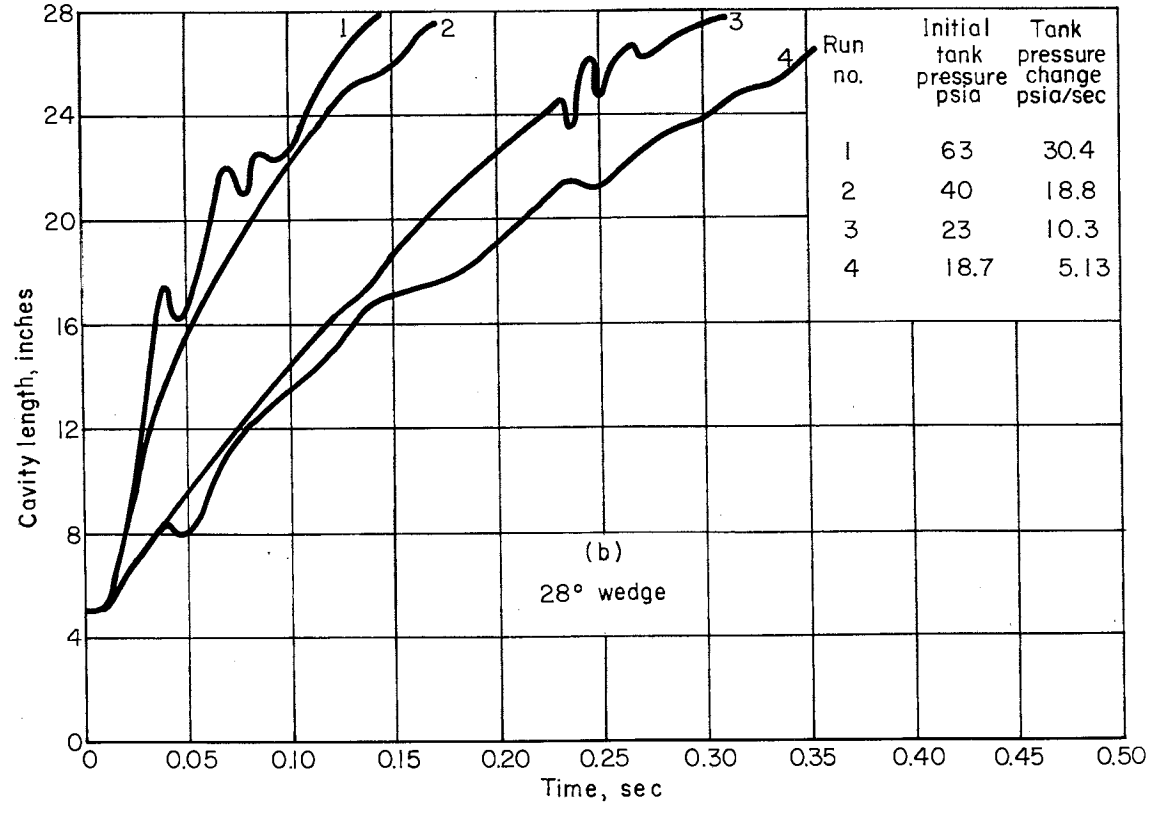

Fig. 24 - Cavity length as a function of time with sudden ventilation

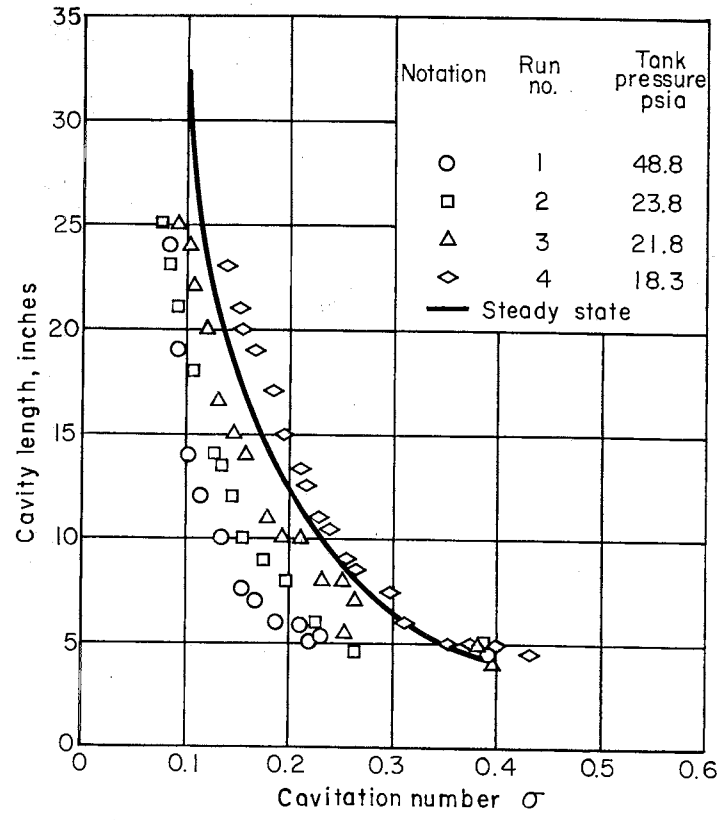

(a) 3/16" normal plate

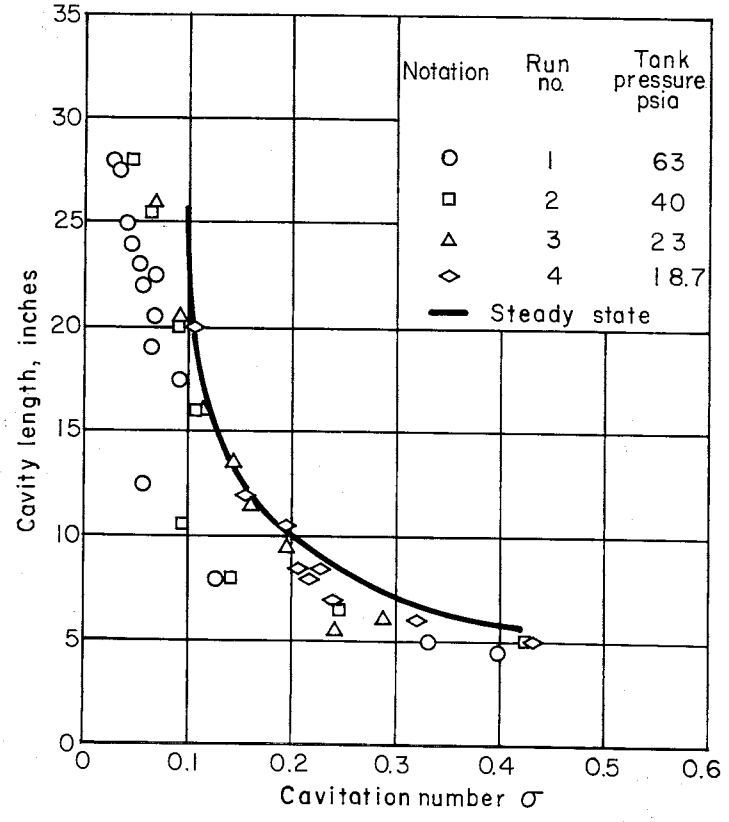

(b) 28° wedge

Fig. 25 - Cavity length as a function of instantaneous cavitation number with sudden ventilation

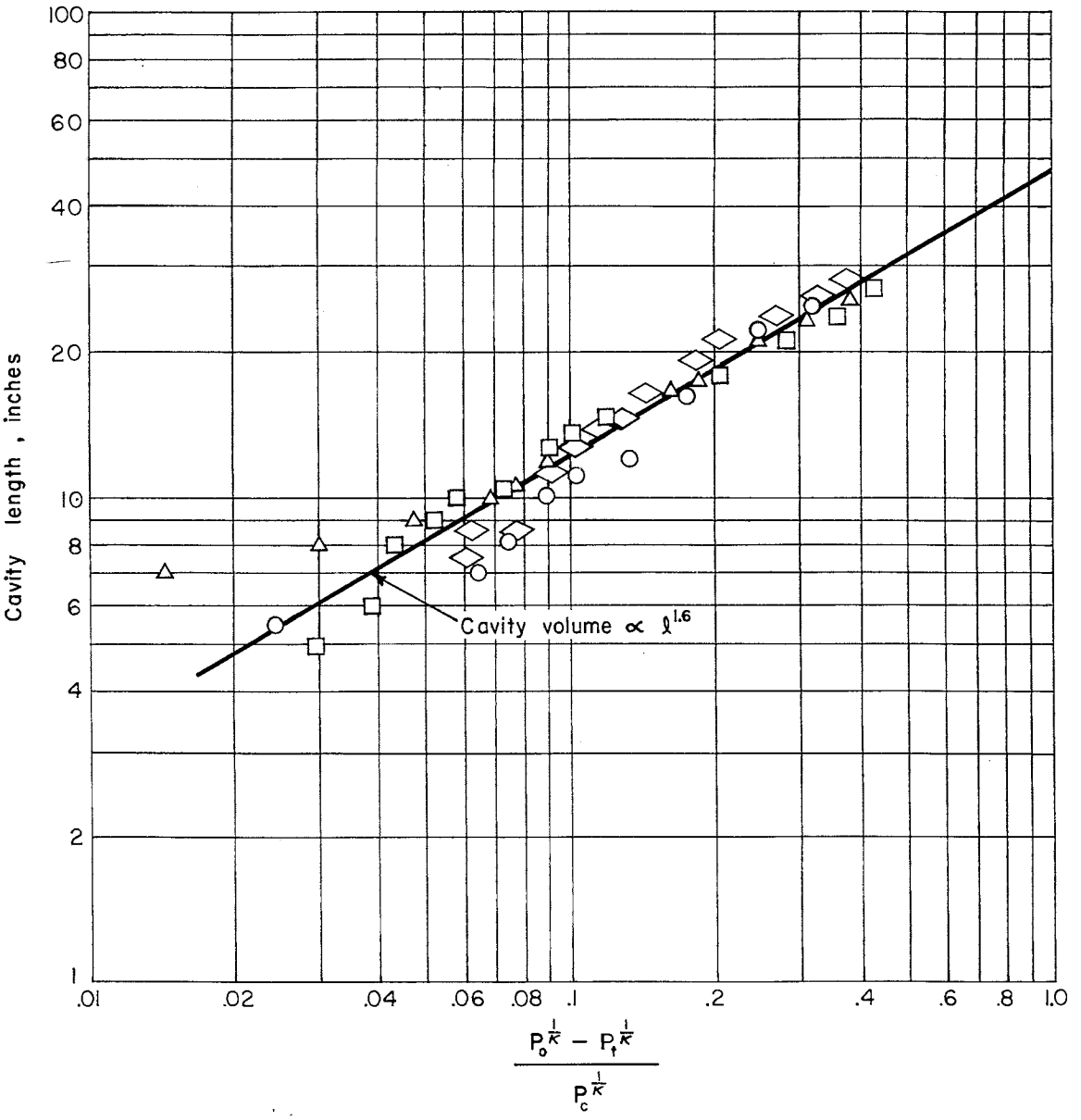

Fig. 26 - Correlation of data for sudden ventilation

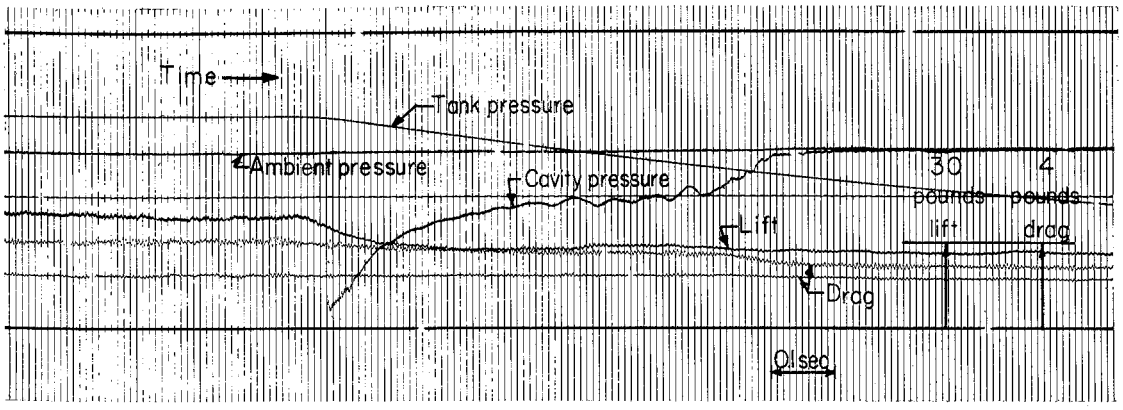

(a) $\alpha = 11^\circ$, $\sigma_v = 0.28$, Initial air tank pressure = 24.3 psia

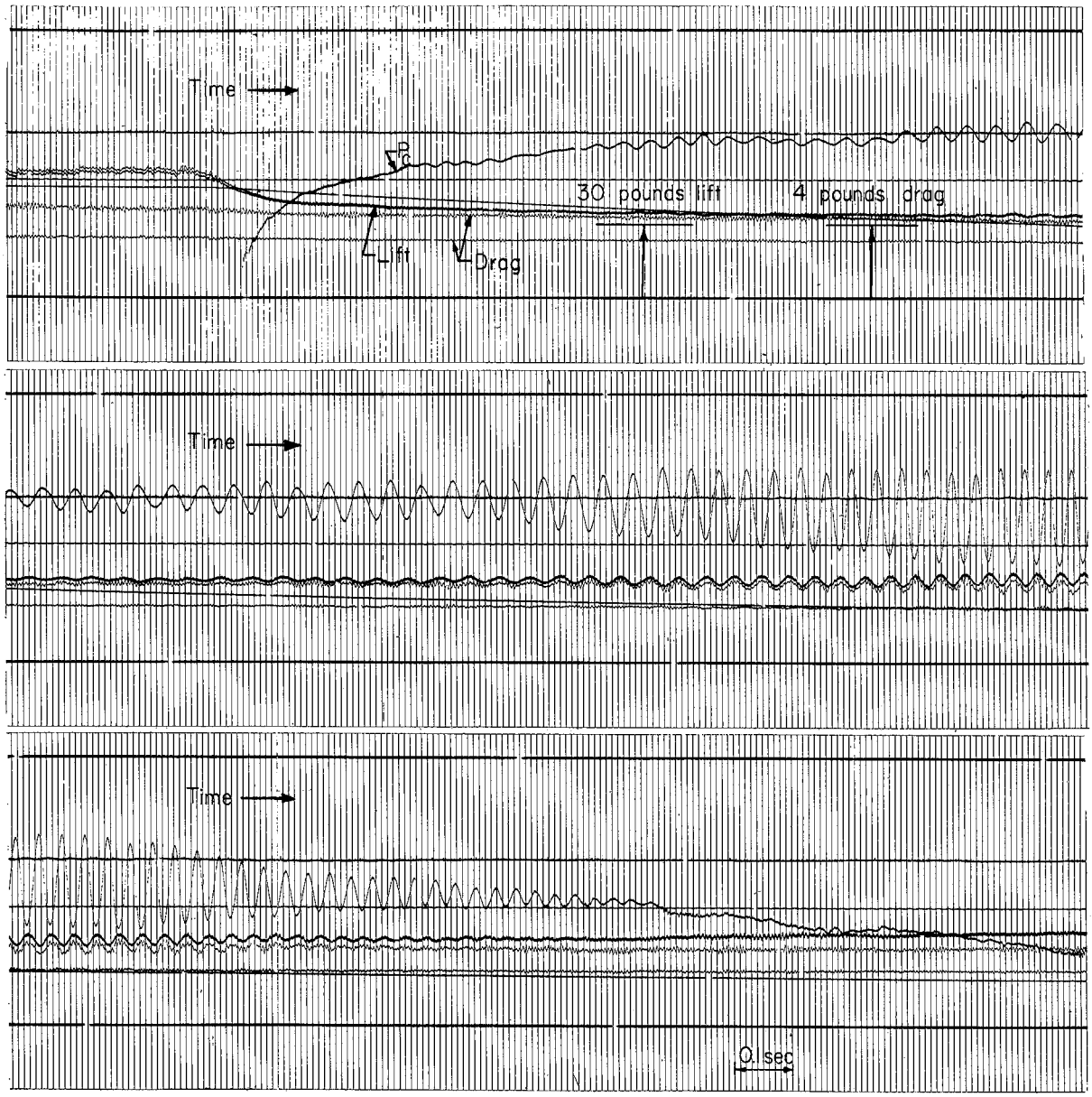

(b) $\alpha = 11^\circ$, $\sigma_v = 0.28$, Initial air tank pressure = 14.3 psia

Fig. 27 - Typical records of lift, drag, and cavity pressure due to sudden ventilation

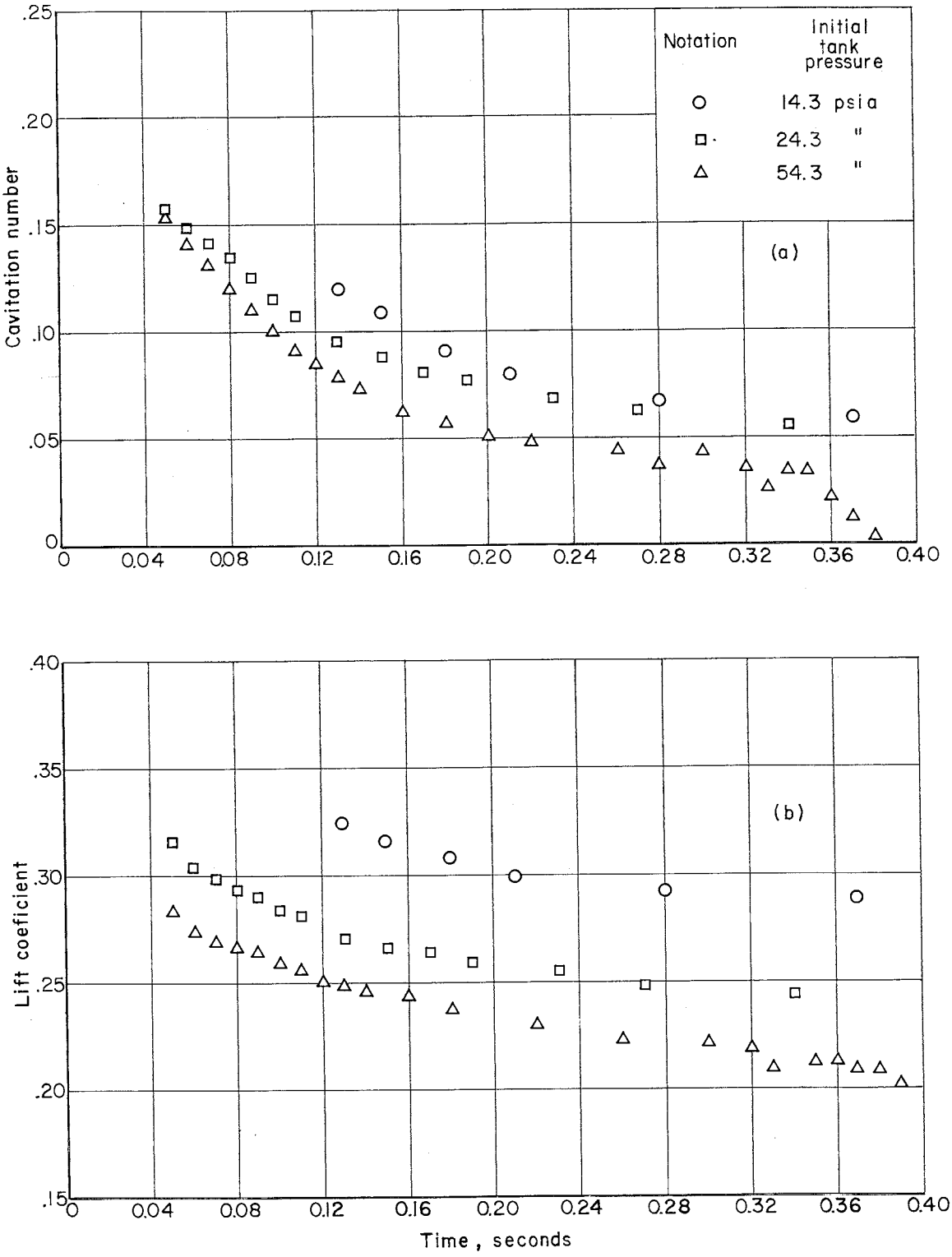

Fig. 28 - Variation of cavitation number and lift coefficient after sudden ventilation

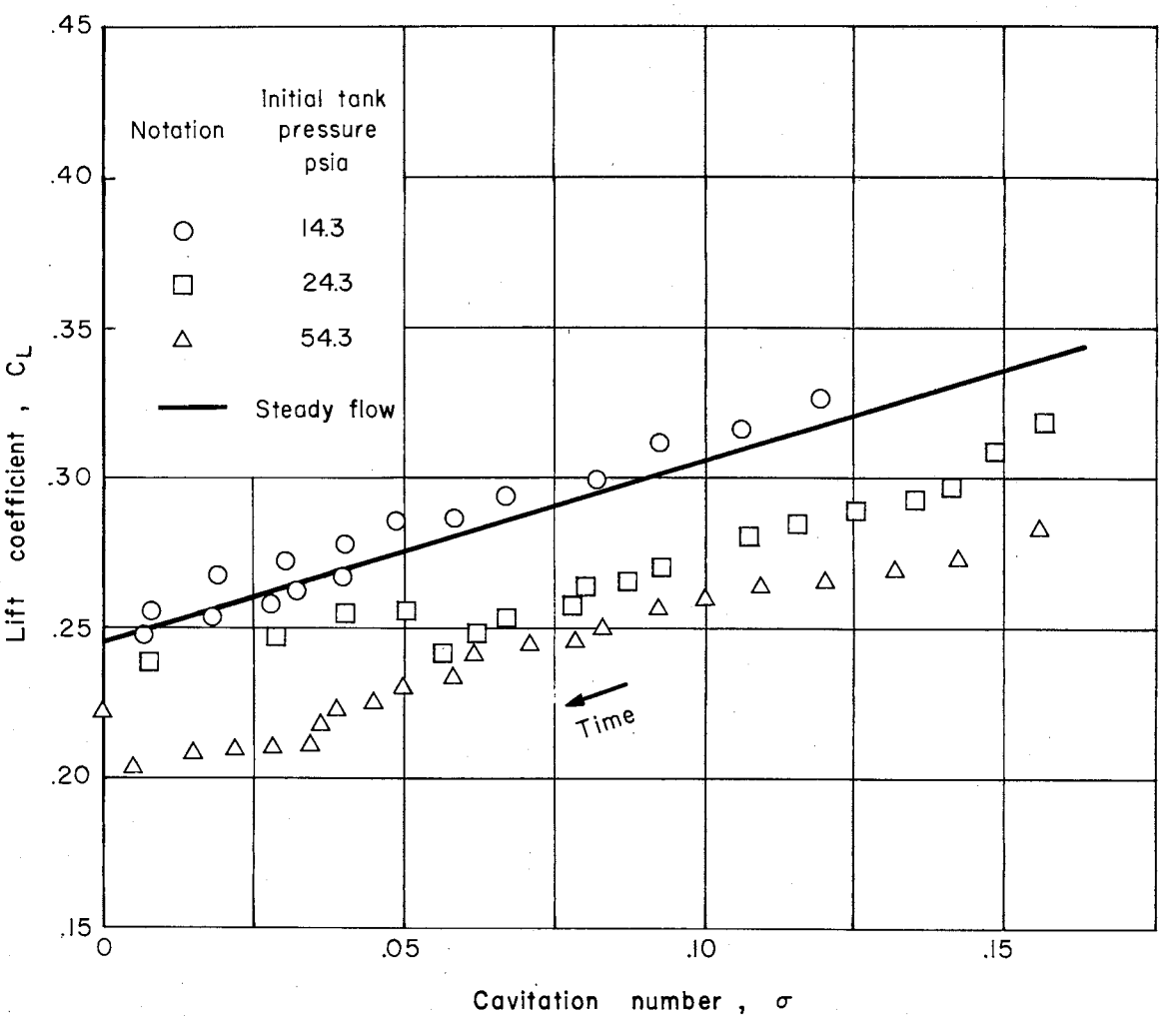

Fig. 29 - Lift coefficient as a function of cavitation number with sudden ventilation

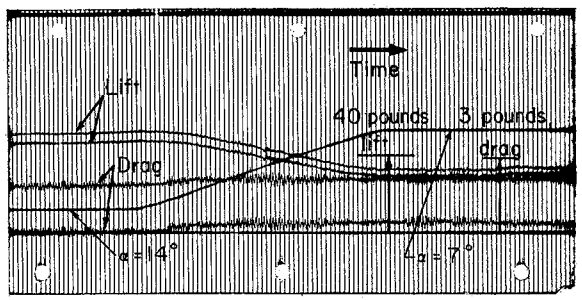

(a) σ = .103 , ℓ_c = 14"~7" , V = 45.3 fps

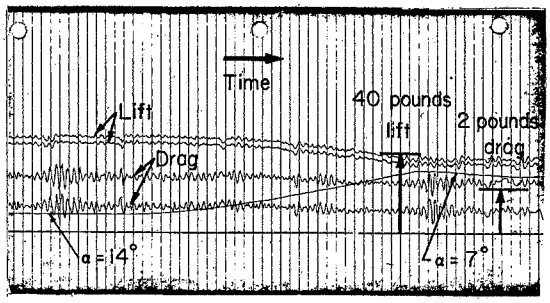

(b) σ = .247 , ℓ_c = 5"~2" , V = 40.6 fps

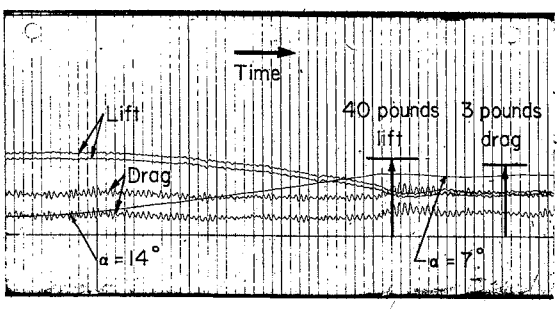

(c) σ = .123 , ℓ_c = 10"~ 4" , V = 42.0 fps

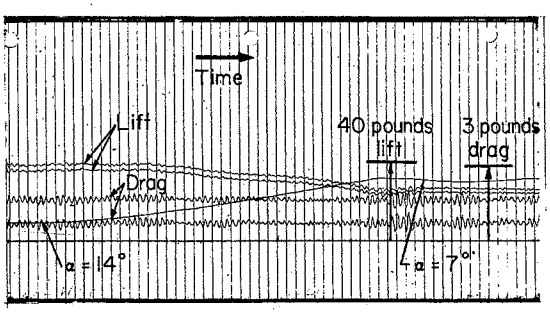

(d) σ = .085 , ℓ_c = 16"~ 7" , V = 42.5 fps

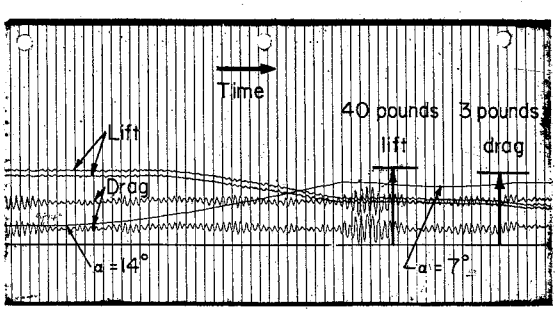

(e) σ = .054 , ℓ_c = 26"~12" , V = 42.9 fps

Fig. 30 - Typical records of lift and drag change after sudden angle of attack change

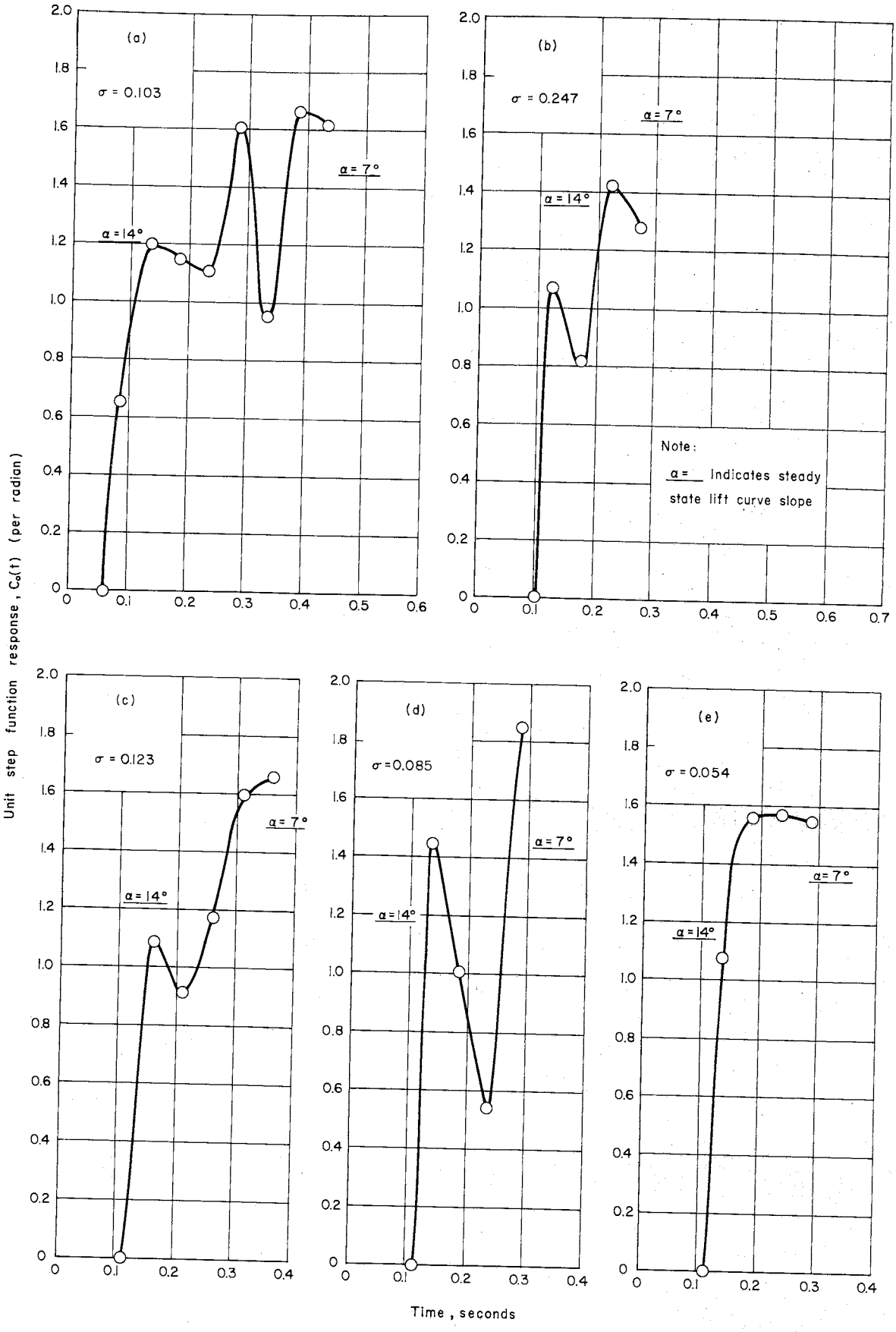

Fig. 31 – The zeroth order unit step function response to angular rotation

SPONSOR'S DISTRIBUTION LIST FOR TECHNICAL PAPER 49-B

of the St. Anthony Falls Hydraulic Laboratory

Copies	Organization
6	Chief of Naval Research, Department of the Navy, Washington, D. C. 20360, Attn: 3 - Code 438 1 - Code 461 1 - Code 463 1 - Code 466
1	Commanding Officer, Office of Naval Research, Branch Office, 495 Summer Street, Boston, Massachusetts.
1	Commanding Officer, Office of Naval Research, Branch Office, 230 N. Michigan Avenue, Chicago 1, Illinois.
1	Commanding Officer, Office of Naval Research, Branch Office, 207 West 24th Street, New York 11, New York.
25	Commanding Officer, Office of Naval Research, Branch Office, Navy No. 100, Box 39, Fleet Post Office, New York, New York.
1	Commanding Officer, Office of Naval Research, Branch Office, 1030 East Green Street, Pasadena 1, California.
1	Commanding Officer, Office of Naval Research, Branch Office, 1000 Geary Street, San Francisco 9, California.
1	Director, Naval Research Laboratory, Washington 25, D. C., Attn: Code 2027.
3	Chief, Bureau of Naval Weapons, Department of the Navy, Washington 25, D. C., Attn: 1 - Code RRRE 1 - Code RAAD 1 - Code RAAD-222
7	Chief, Bureau of Ships, Department of the Navy, Washington 25, D. C. Attn: 1 - Code 312 1 - Code 335 1 - Code 420 1 - Code 421 1 - Code 440 1 - Code 442 1 - Code 449
1	Chief, Bureau of Yards and Docks, Department of the Navy, Washington 25, D. C. Attn: Code D-400.
12	Commanding Officer and Director, David Taylor Model Basin, Washington 7, D. C., Attn: 1 - Code 500 1 - Code 513

Copies	Organization
	1 - Code 520 1 - Code 525 1 - Code 526 1 - Code 526A 1 - Code 530 1 - Code 533 1 - Code 580 1 - Code 585 1 - Code 589 1 - Code 700
1	Commander, Naval Ordnance Test Station, China Lake, California, Attn: Code 753.
1	Commander, Naval Ordnance Test Station, Pasadena Annex, 3202 E. Foothill Boulevard, Pasadena 8, California, Attn: Code P508.
1	Commander, Portsmouth Naval Shipyard, Portsmouth, New Hampshire, Attn: Planning Department.
1	Commander, Boston Naval Shipyard, Boston, Massachusetts, Attn: Planning Department.
1	Commander, Pearl Harbor Naval Shipyard, Navy No. 128, Fleet Post Office, San Francisco, California, Attn: Planning Department.
1	Commander, San Francisco Naval Shipyard, San Francisco, California, Attn: Planning Department.
1	Commander, Mare Island Naval Shipyard, Vallejo, California, Attn: Planning Department.
1	Commander, New York Naval Shipyard, Brooklyn 1, New York, Attn: Planning Department.
1	Commander, Puget Sound Naval Shipyard, Bremerton, Washington, Attn: Planning Department.
1	Commander, Philadelphia Naval Shipyard, Philadelphia, Pennsylvania, Attn: Planning Department.
1	Commander, Norfolk Naval Shipyard, Portsmouth, Virginia, Attn: Planning Department.
1	Commander, Charleston Naval Shipyard, Charleston, South Carolina, Attn: Planning Department.
1	Commander, Long Beach Naval Shipyard, Long Beach 2, California, Attn: Planning Department.
1	Commander, US Naval Weapons Laboratory, Dahlgren, Virginia, Attn: Planning Department.
1	Commander, US Naval Ordnance Laboratory, White Oak, Maryland.
1	Commander, US Naval Weapons Laboratory, Dahlgren, Virginia, Attn: Computation and Exterior Ballistics Laboratory (Dr. A. V. Hershey).
1	Superintendent, US Naval Academy, Annapolis, Maryland, Attn: Library.

Copies	Organization
1	Superintendent, US Naval Postgraduate School, Monterey, California.
1	Commandant, US Coast Guard, 1300 E Street, NW, Washington, D.C.
1	Secretary, Ship Structure Committee, US Coast Guard Headquarters, 1300 E Street, NW, Washington, D.C.
1	Commander, Military Sea Transportation Service, Department of the Navy, Washington 25, D. C.
1	Division of Ship Design, Maritime Administration, 441 G Street, NW, Washington 25, D. C.
1	Superintendent, US Merchant Marine Academy, Kings Point, Long Island, New York, Attn: Captain L. S. McCready.
1	Commanding Officer and Director, US Navy Mine Defense Laboratory, Panama City, Florida.
1	Commanding Officer, NROTC and Naval Administrative Unit, Massachusetts Institute of Technology, Cambridge 39, Massachusetts.
1	Commander, Hdqs. US Army Transportation Research and Development Command, Transportation Corps, Fort Eustis, Virginia, Attn: Marine Transportation Division.
1	Air Force Office of Scientific Research, Mechanics Division, Washington 25, D. C.
1	Commander, Wright Air Development Division, Aircraft Laboratory, Wright-Patterson Air Force Base, Ohio, Attn: Mr. W. Mykytow, Dynamics Branch.
1	Director of Research, Code RR, National Aeronautics and Space Administration, 600 Independence Avenue, SW, Washington, D. C. 20546.
1	Director, Langley Research Center, Langley Station, Hampton, Virginia, Attn: Mr. I. E. Garrick.
1	Director, Langley Research Center, Langley Station, Hampton, Virginia, Attn: Mr. D. J. Marten.
1	Director, Engineering Science Division, National Science Foundation, Washington, D. C.
1	Director, National Bureau of Standards, Washington 25, D. C., Attn: Mr. J. M. Franklin.
1	Dr. G. B. Schubauer, Fluid Mechanics Section, National Bureau of Standards, Washington 25, D. C.
20	Defense Documentation Center, Cameron Station, Alexandria, Virginia.
1	Office of Technical Services, Department of Commerce, Washington 25, D. C.
1	Mr. Alfonso Alcadan L., Director, Laboratorio Nacional de Hydraulica, Antiguo Camino A Ancon, Casialla Postal, 682, Lima, Peru.
1	Mr. T. A. Duncan, Lycoming Division, AVCO Corporation, 1701 K Street, NW, Apartment 904, Washington, D. C.

Copies	Organization
1	Baker Manufacturing Company, Evansville, Wisconsin.
1	Professor S. Siestrunck, Bureau D'Analyse et de Recherche Appliquees, 47, Avenue Victor Cresson, Issy-les-Moulineaux, Seine, France.
1	Professor A. Acosta, California Institute of Technology, Pasadena 4, California.
1	Professor M. Plesset, California Institute of Technology, Pasadena 4, California.
1	Professor T. Y. Wu, California Institute of Technology, Pasadena 4, California.
1	Professor A. Powell, University of California, Los Angeles, California.
1	Dr. Maurice L. Albertson, Professor of Civil Engineering, Colorado State University, Fort Collins, Colorado 80521.
1	Professor J. E. Cermak, Colorado State University, Department of Civil Engineering, Fort Collins, Colorado.
1	Dr. Blaine R. Parkin, General Dynamics - Convair, P. O. Box 1950, San Diego 12, California.
1	Robert H. Oversmith, Chief of ASW/Marine Sciences, Mail Zone 6-107, General Dynamics - Convair, San Diego, California 92112.
1	Dr. Irving C. Statler, Head, Applied Mechanics Department, Cornell Aeronautical Laboratory, Inc., P. O. Box 235, Buffalo, New York 14221.
1	Mr. Richard P. White, Jr., Cornell Aeronautical Laboratory, 4455 Genesee Street, Buffalo, New York.
1	Professor W. R. Sears, Graduate School of Aeronautical Engineering, Cornell University, Ithaca, New York.
1	Mr. George H. Pedersen, Curtiss-Wright Corporation, Wright Aeronautical Division, Wood-Ridge, New Jersey, Location CC-1 Engrg. Mezz.
1	Mr. G. Tedrew, Food Machinery Corporation, P. O. Box 367, San Jose, California.
1	General Applied Science Laboratory, Merrick and Stewart Avenues, Westbury, Long Island, New York, Attn: Dr. Frank Lane.
1	Mr. R. McCandliss, Electric Boat Division, General Dynamics Corporation, Groton, Connecticut.
1	Dr. A. S. Iberall, President, General Technical Services, Inc., 2640 Whiton Road, Cleveland 18, Ohio.
1	Gibbs and Cox, Inc., 21 West Street, New York, New York 10006.
1	Mr. Eugene F. Baird, Chief of Dynamic Analysis, Grumman Aircraft Engineering Corporation, Bethpage Long Island, New York.

Copies	Organization
1	Mr. Robert E. Bower, Chief, Advanced Development, Grumman Aircraft Engineering Corporation, Bethpage, Long Island, New York.
1	Mr. William P. Carl, Grumman Aircraft Engineering Corporation, Bethpage, Long Island, New York.
1	Grumman Aircraft Engineering Corporation, Research Department, Plant 25, Bethpage, Long Island, New York 11714, Attn: Mr. Kenneth Keen.
1	Dr. O. Grim, Hamburgische Schiffbau-Versuchsanstalt, Bramfelder Strasse 164, Hamburg 33, Germany.
1	Dr. H. W. Lerbs, Hamburgische Schiffbau-Versuchsanstalt, Bramfelder Strasse 164, Hamburg 33, Germany.
1	Dr. H. Schwanecke, Hamburgische Schiffbau-Versuchsanstalt, Bramfelder Strasse 164, Hamburg 33, Germany.
1	Professor G. P. Weinblum, Director, Institute for Schiffbau, University of Hamburg, Berliner Tow 21, Hamburg, Germany.
1	Professor G. F. Carrier, Harvard University, Cambridge 38, Massachusetts.
1	Dr. S. F. Hoerner, 148 Busteed Drive, Midland Park, New Jersey.
1	Mr. P. Eisenbert, President, Hydronautics, Incorporated, Pindell School Road, Howard County, Laurel, Maryland.
1	Professor Carl Prohaska, Hydro-og Aerodynamisk Laboratorium, Lyngby, Denmark.
1	Professor L. Landweber, Iowa Institute of Hydraulic Research, State University of Iowa, Iowa City, Iowa.
1	Professor H. Rouse, Iowa Institute of Hydraulic Research, State University of Iowa, Iowa City, Iowa.
1	Professor S. Corrsin, Department of Mechanics, The Johns Hopkins University, Baltimore 18, Maryland.
2	Professor O. M. Phillips, Division of Mechanical Engineering, Institute for Cooperative Research, The Johns Hopkins University, Baltimore 18, Maryland.
1	Mr. Bill East, Lockheed Aircraft Corporation, California Division, Hydrodynamics Research, Burbank, California.
1	Mr. R. W. Kermeen, Lockheed Missiles and Space Company, Department 81-73/Bldg. 538, P. O. Box 504, Sunnyvale, California.
1	Department of Naval Architecture and Marine Engineering, Room 5-228, Massachusetts Institute of Technology, 77 Massachusetts Avenue, Cambridge, Massachusetts 02139.
1	Professor M. A. Abkowitz, Massachusetts Institute of Technology, Cambridge 39, Massachusetts.

Copies	Organization
1	Professor H. Ashley, Massachusetts Institute of Technology, Cambridge 39, Massachusetts.
1	Professor A. T. Ippen, Massachusetts Institute of Technology, Cambridge 39, Massachusetts.
1	Professor M. Landahl, Massachusetts Institute of Technology, Cambridge 39, Massachusetts.
1	Dr. H. Reichardt, Director, Max-Planck Institut fur Stromungsforschung, Bottingerstrasse 6-8, Gottingen, Germany.
1	Professor R. B. Couch, University of Michigan, Ann Arbor, Michigan.
1	Professor W. W. Willmarth, University of Michigan, Ann Arbor, Michigan.
1	Midwest Research Institute, 425 Volker Boulevard, Kansas City, Missouri, Attn: Library.
1	Director, St. Anthony Falls Hydraulic Laboratory, University of Minnesota, Minneapolis 14, Minnesota.
1	Mr. C. S. Song, St. Anthony Falls Hydraulic Laboratory, University of Minnesota, Minneapolis 14, Minnesota.
1	Mr. J. M. Wetzel, St. Anthony Falls Hydraulic Laboratory, University of Minnesota, Minneapolis 14, Minnesota.
1	Head, Aerodynamics Division, National Physical Laboratory, Teddington, Middlesex, England.
1	Mr. A.Silverleaf, National Physical Laboratory, Teddington,Middlesex, England.
1	The Aeronautical Library, National Research Council, Montreal Road, Ottawa 2, Canada.
1	Dr. J. B. Van Manen, Netherlands Ship Model Basin, Wageningen, The Netherlands.
1	Professor John J. Foody, Chairman, Engineering Department, State University of New York, Maritime College, Bronx, New York 10465.
1	Professor J. Keller, Institute of Mathematical Sciences, New York University, 25 Waverly Place, New York 3, New York.
1	Professor J. J. Stoker, Institute of Mathematical Sciences, New York University, 25 Waverly Place, New York 3, New York.
1	Dr. T. R. Goodman, Oceanics, Incorporated, Technical Industrial Park, Plainview, Long Island, New York.
1	Professor J. William Holl, Department of Aeronautical Engineering, The Pennsylvania State University, Ordnance Research Laboratory, P. O. Box 30, State College, Pennsylvania.
1	Dr. M. Sevik, Ordnance Research Laboratory, Pennsylvania State University, University Park, Pennsylvania.

Copies	Organization
1	Dr. George F. Wislicenus, Garfield Thomas Water Tunnel, Ordnance Research Laboratory, The Pennsylvania State University, Post Office Box 30, State College, Pennsylvania 16801.
1	Professor E. J. Brunelle, Princeton University, Princeton, New Jersey.
1	Mr. David Wellinger, Hydrofoil Projects, Radio Corporation of America, Burlington, Massachusetts.
1	The RAND Corporation, 1700 Main Street, Santa Monica, California, 90406, Attn: Library.
1	Professor R. C. DiPrima, Department of Mathematics, Rensselaer Polytechnic Institute, Troy, New York.
1	Mr. L. M. White, U. S. Rubber Company, Research and Development Department, Wayne, New Jersey.
1	Professor J. K. Lunde, Skipsmodelltanken, Trondheim, Norway.
1	Editor, Applied Mechanics Review, Southwest Reseaech Institute, 8500 Culebra Road, San Antonio 6, Texas.
1	Dr. H. N. Abramson, Southwest Research Institute, 8500 Culebra Road, San Antonio 6, Texas.
1	Mr. G. Ransleben, Southwest Research Institute, 8500 Culebra Road, San Antonio 6, Texas.
1	Professor E. Y. Hsu, Stanford University, Stanford, California.
1	Dr. Byrne Perry, Department of Civil Engineering, Stanford University, Stanford, California 94305.
1	Mr. J. P. Breslin, Stevens Institute of Technology, Davidson Laboratory, Hoboken, New Jersey.
1	Mr. D. Savitsky, Stevens Institute of Technology, Davidson Laboratory, Hoboken, New Jersey.
1	Mr. S. Tsakonas, Stevens Institute of Technology, Davidson Laboratory, Hoboken, New Jersey.
1	Dr. Jack Kotik, Technical Research Group, Inc., Route 110, Melville, New York.
1	Dr. R. Timman, Department of Applied Mathematics, Technological University, Julianalaan, Delft, Holland.
1	Transportation Technical Research Institute, No. 1057-1 Chome, Mejiromachi, Toshima-ku, Tokyo-to, Japan.
1	Dr. Grosse, Versuchsanstalt fur Wasserbau und Schiffbau, Schleuseninsel im Tiergarten, Berlin, Germany.
1	Dr. S. Schuster, Director, Versuchsanstalt fur Wasserbau und Schiffbau, Schleuseninsel im Tiergarten, Berlin, Germany.

Copies	Organization
1	Technical Library, Webb Institute of Naval Architecture, Glen Cove, Long Island, New York.
1	Professor E. V. Lewis, Webb Institute of Naval Architecture, Glen Cove, Long Island, New York.
1	Mr. C. Wigley, Flat 103, 6-9 Charterhouse Square, London E. C. 1, England.
1	Coordinator of Research, Maritime Administration, 441 G Street, NW, Washington 25, D. C.

Technical Paper No. 49, Series B
St. Anthony Falls Hydraulic Laboratory

MEASUREMENTS OF THE UNSTEADY FORCE ON CAVITATING HYDROFOILS IN A FREE JET, by C. S. Song. June 1964. 55 pages incl. 31 illus. Contract Nonr 710(24).

Experimental data concerning force and other related quantities associated with unsteady supercavitating flow about bodies tested in a free-jet water tunnel are reported herein. Three types of unsteady flows were studied -- those due to pitching oscillation, sudden ventilation, and sudden angle of attack change. All test bodies were of such geometrical configuration that separation could occur only at two or three fixed points.

Available from St. Anthony Falls Hydraulic Laboratory, University of Minnesota, at $1.75 per copy.

UNCLASSIFIED

1. Cavitation
2. Hydrofoil
3. Supercavitating Foil
4. Oscillating Foil
5. Free-Surface Effect

I. Title
II. Song, C. S.
III. St. Anthony Falls Hydraulic Laboratory
IV. Contract No. 710(24)

Technical Paper No. 49, Series B
St. Anthony Falls Hydraulic Laboratory

MEASUREMENTS OF THE UNSTEADY FORCE ON CAVITATING HYDROFOILS IN A FREE JET, by C. S. Song. June 1964. 55 pages incl. 31 illus. Contract Nonr 710(24).

Experimental data concerning force and other related quantities associated with unsteady supercavitating flow about bodies tested in a free-jet water tunnel are reported herein. Three types of unsteady flows were studied -- those due to pitching oscillation, sudden ventilation, and sudden angle of attack change. All test bodies were of such geometrical configuration that separation could occur only at two or three fixed points.

Available from St. Anthony Falls Hydraulic Laboratory, University of Minnesota, at $1.75 per copy.

UNCLASSIFIED

1. Cavitation
2. Hydrofoil
3. Supercavitating Foil
4. Oscillating Foil
5. Free-Surface Effect

I. Title
II. Song, C. S.
III. St. Anthony Falls Hydraulic Laboratory
IV. Contract No. 710(24)

Technical Paper No. 49, Series B
St. Anthony Falls Hydraulic Laboratory

MEASUREMENTS OF THE UNSTEADY FORCE ON CAVITATING HYDROFOILS IN A FREE JET, by C. S. Song. June 1964. 55 pages incl. 31 illus. Contract Nonr 710(24).

Experimental data concerning force and other related quantities associated with unsteady supercavitating flow about bodies tested in a free-jet water tunnel are reported herein. Three types of unsteady flows were studied -- those due to pitching oscillation, sudden ventilation, and sudden angle of attack change. All test bodies were of such geometrical configuration that separation could occur only at two or three fixed points.

Available from St. Anthony Falls Hydraulic Laboratory, University of Minnesota, at $1.75 per copy.

UNCLASSIFIED

1. Cavitation
2. Hydrofoil
3. Supercavitating Foil
4. Oscillating Foil
5. Free-Surface Effect

I. Title
II. Song, C. S.
III. St. Anthony Falls Hydraulic Laboratory
IV. Contract No. 710(24)

Technical Paper No. 49, Series B
St. Anthony Falls Hydraulic Laboratory

MEASUREMENTS OF THE UNSTEADY FORCE ON CAVITATING HYDROFOILS IN A FREE JET, by C. S. Song. June 1964. 55 pages incl. 31 illus. Contract Nonr 710(24).

Experimental data concerning force and other related quantities associated with unsteady supercavitating flow about bodies tested in a free-jet water tunnel are reported herein. Three types of unsteady flows were studied -- those due to pitching oscillation, sudden ventilation, and sudden angle of attack change. All test bodies were of such geometrical configuration that separation could occur only at two or three fixed points.

Available from St. Anthony Falls Hydraulic Laboratory, University of Minnesota, at $1.75 per copy.

UNCLASSIFIED

1. Cavitation
2. Hydrofoil
3. Supercavitating Foil
4. Oscillating Foil
5. Free-Surface Effect

I. Title
II. Song, C. S.
III. St. Anthony Falls Hydraulic Laboratory
IV. Contract No. 710(24)

Technical Paper No. 49, Series B
St. Anthony Falls Hydraulic Laboratory

MEASUREMENTS OF THE UNSTEADY FORCE ON CAVITATING HYDROFOILS IN A FREE JET, by C. S. Song. June 1964. 55 pages incl. 31 illus. Contract Nonr 710(24).

Experimental data concerning force and other related quantities associated with unsteady supercavitating flow about bodies tested in a free-jet water tunnel are reported herein. Three types of unsteady flows were studied -- those due to pitching oscillation, sudden ventilation, and sudden angle of attack change. All test bodies were of such geometrical configuration that separation could occur only at two or three fixed points.

Available from St. Anthony Falls Hydraulic Laboratory, University of Minnesota, at $1.75 per copy.

UNCLASSIFIED

1. Cavitation
2. Hydrofoil
3. Supercavitating Foil
4. Oscillating Foil
5. Free-Surface Effect

I. Title
II. Song, C. S.
III. St. Anthony Falls Hydraulic Laboratory
IV. Contract No. 710(24)

Technical Paper No. 49, Series B
St. Anthony Falls Hydraulic Laboratory

MEASUREMENTS OF THE UNSTEADY FORCE ON CAVITATING HYDROFOILS IN A FREE JET, by C. S. Song. June 1964. 55 pages incl. 31 illus. Contract Nonr 710(24).

Experimental data concerning force and other related quantities associated with unsteady supercavitating flow about bodies tested in a free-jet water tunnel are reported herein. Three types of unsteady flows were studied -- those due to pitching oscillation, sudden ventilation, and sudden angle of attack change. All test bodies were of such geometrical configuration that separation could occur only at two or three fixed points.

Available from St. Anthony Falls Hydraulic Laboratory, University of Minnesota, at $1.75 per copy.

UNCLASSIFIED

1. Cavitation
2. Hydrofoil
3. Supercavitating Foil
4. Oscillating Foil
5. Free-Surface Effect

I. Title
II. Song, C. S.
III. St. Anthony Falls Hydraulic Laboratory
IV. Contract No. 710(24)

Technical Paper No. 49, Series B
St. Anthony Falls Hydraulic Laboratory

MEASUREMENTS OF THE UNSTEADY FORCE ON CAVITATING HYDROFOILS IN A FREE JET, by C. S. Song. June 1964. 55 pages incl. 31 illus. Contract Nonr 710(24).

Experimental data concerning force and other related quantities associated with unsteady supercavitating flow about bodies tested in a free-jet water tunnel are reported herein. Three types of unsteady flows were studied -- those due to pitching oscillation, sudden ventilation, and sudden angle of attack change. All test bodies were of such geometrical configuration that separation could occur only at two or three fixed points.

Available from St. Anthony Falls Hydraulic Laboratory, University of Minnesota, at $1.75 per copy.

UNCLASSIFIED

1. Cavitation
2. Hydrofoil
3. Supercavitating Foil
4. Oscillating Foil
5. Free-Surface Effect

I. Title
II. Song, C. S.
III. St. Anthony Falls Hydraulic Laboratory
IV. Contract No. 710(24)

Technical Paper No. 49, Series B
St. Anthony Falls Hydraulic Laboratory

MEASUREMENTS OF THE UNSTEADY FORCE ON CAVITATING HYDROFOILS IN A FREE JET, by C. S. Song. June 1964. 55 pages incl. 31 illus. Contract Nonr 710(24).

Experimental data concerning force and other related quantities associated with unsteady supercavitating flow about bodies tested in a free-jet water tunnel are reported herein. Three types of unsteady flows were studied -- those due to pitching oscillation, sudden ventilation, and sudden angle of attack change. All test bodies were of such geometrical configuration that separation could occur only at two or three fixed points.

Available from St. Anthony Falls Hydraulic Laboratory, University of Minnesota, at $1.75 per copy.

UNCLASSIFIED

1. Cavitation
2. Hydrofoil
3. Supercavitating Foil
4. Oscillating Foil
5. Free-Surface Effect

I. Title
II. Song, C. S.
III. St. Anthony Falls Hydraulic Laboratory
IV. Contract No. 710(24)

Technical Paper No. 49, Series B
St. Anthony Falls Hydraulic Laboratory

MEASUREMENTS OF THE UNSTEADY FORCE ON CAVITATING HYDROFOILS IN A FREE JET, by C. S. Song. June 1964. 55 pages incl. 31 illus. Contract Nonr 710(24).

Experimental data concerning force and other related quantities associated with unsteady supercavitating flow about bodies tested in a free-jet water tunnel are reported herein. Three types of unsteady flows were studied -- those due to pitching oscillation, sudden ventilation, and sudden angle of attack change. All test bodies were of such geometrical configuration that separation could occur only at two or three fixed points.

Available from St. Anthony Falls Hydraulic Laboratory, University of Minnesota, at $1.75 per copy.

UNCLASSIFIED

1. Cavitation
2. Hydrofoil
3. Supercavitating Foil
4. Oscillating Foil
5. Free-Surface Effect

I. Title
II. Song, C. S.
III. St. Anthony Falls Hydraulic Laboratory
IV. Contract No. 710(24)

Technical Paper No. 49, Series B
St. Anthony Falls Hydraulic Laboratory

MEASUREMENTS OF THE UNSTEADY FORCE ON CAVITATING HYDROFOILS IN A FREE JET, by C. S. Song. June 1964. 55 pages incl. 31 illus. Contract Nonr 710(24).

Experimental data concerning force and other related quantities associated with unsteady supercavitating flow about bodies tested in a free-jet water tunnel are reported herein. Three types of unsteady flows were studied -- those due to pitching oscillation, sudden ventilation, and sudden angle of attack change. All test bodies were of such geometrical configuration that separation could occur only at two or three fixed points.

Available from St. Anthony Falls Hydraulic Laboratory, University of Minnesota, at $1.75 per copy.

UNCLASSIFIED

1. Cavitation
2. Hydrofoil
3. Supercavitating Foil
4. Oscillating Foil
5. Free-Surface Effect

I. Title
II. Song, C. S.
III. St. Anthony Falls Hydraulic Laboratory
IV. Contract No. 710(24)

Technical Paper No. 49, Series B
St. Anthony Falls Hydraulic Laboratory

MEASUREMENTS OF THE UNSTEADY FORCE ON CAVITATING HYDROFOILS IN A FREE JET, by C. S. Song. June 1964. 55 pages incl. 31 illus. Contract Nonr 710(24).

Experimental data concerning force and other related quantities associated with unsteady supercavitating flow about bodies tested in a free-jet water tunnel are reported herein. Three types of unsteady flows were studied -- those due to pitching oscillation, sudden ventilation, and sudden angle of attack change. All test bodies were of such geometrical configuration that separation could occur only at two or three fixed points.

Available from St. Anthony Falls Hydraulic Laboratory, University of Minnesota, at $1.75 per copy.

UNCLASSIFIED

1. Cavitation
2. Hydrofoil
3. Supercavitating Foil
4. Oscillating Foil
5. Free-Surface Effect

I. Title
II. Song, C. S.
III. St. Anthony Falls Hydraulic Laboratory
IV. Contract No. 710(24)

Technical Paper No. 49, Series B
St. Anthony Falls Hydraulic Laboratory

MEASUREMENTS OF THE UNSTEADY FORCE ON CAVITATING HYDROFOILS IN A FREE JET, by C. S. Song. June 1964. 55 pages incl. 31 illus. Contract Nonr 710(24).

Experimental data concerning force and other related quantities associated with unsteady supercavitating flow about bodies tested in a free-jet water tunnel are reported herein. Three types of unsteady flows were studied -- those due to pitching oscillation, sudden ventilation, and sudden angle of attack change. All test bodies were of such geometrical configuration that separation could occur only at two or three fixed points.

Available from St. Anthony Falls Hydraulic Laboratory, University of Minnesota, at $1.75 per copy.

UNCLASSIFIED

1. Cavitation
2. Hydrofoil
3. Supercavitating Foil
4. Oscillating Foil
5. Free-Surface Effect

I. Title
II. Song, C. S.
III. St. Anthony Falls Hydraulic Laboratory
IV. Contract No. 710(24)